https://ntrs.nasa.gov/search.jsp?R=19910008720 2020-03-19T19:37:02+00:00Z

X91-36001

X91-36001*

nasa pers. only

NASA Technical Memorandum 4250

Low-Speed Wind-Tunnel Test of an Unpowered High-Speed Stoppable Rotor Concept in Fixed-Wing Mode

Michael B. Lance, Daniel Y. Sung,
and Robert H. Stroub

MARCH 1991

NASA

NASA Technical Memorandum 4250

Low-Speed Wind-Tunnel Test of an Unpowered High-Speed Stoppable Rotor Concept in Fixed-Wing Mode

Michael B. Lance
Lockheed Engineering & Sciences Company
Hampton, Virginia

Daniel Y. Sung
Sterling Software
Palo Alto, California

Robert H. Stroub
Ames Research Center
Moffett Field, California

National Aeronautics and
Space Administration
Office of Management
Scientific and Technical
Information Division

1991

Summary

An experimental investigation of the M85, a high-speed rotor concept, was conducted in the Langley 14- by 22-Foot Subsonic Tunnel in cooperation with NASA Ames Research Center. An unpowered 1/5-scale model of the XH-59A helicopter fuselage with a large circular hub fairing, two rotor blades, and a shaft fairing was used as a baseline configuration. The M85 is a rotor-wing hybrid aircraft design, and the model was tested with the rotor blades in the fixed-wing mode. Assessments of the aerodynamic characteristics of various model rotor configurations were made. Variations in configuration were produced by changing the rotor blade sweep angle, the blade chord length, the shaft fairing, and the port-blade leading-edge orientation. The configuration that included wide-chord blades at a sweep angle of 0° appeared to be the most favorable of all the configurations tested.

Introduction

Historically, there have been many attempts to produce an aircraft that would economically combine the desirable properties of both the helicopter and the fixed-wing aircraft (refs. 1–6). A proposed configuration for such an aircraft is the M85 high-speed rotor concept. The M85, which is a stoppable rotor-wing hybrid aircraft concept, would be able to hover efficiently and attain a cruise speed in excess of 500 knots.

A unique feature of the M85 concept is the lifting system. The M85 would incorporate three or four rotor blades mounted on a central circular platform, which would be mounted on a shaft fairing. In hover and low-speed flight, the central platform and blades would rotate. Prior to high-speed flight, the blades would be retracted, and central platform rotation would be stopped. Flying on central platform lift alone, the aircraft would accelerate to cruise speed. At cruise speed, selected blades would be redeployed to act as wings for additional lift.

An investigation of the low-speed, fixed-wing aerodynamic characteristics of the M85 high-speed rotor concept was conducted in the Langley 14- by 22-Foot Subsonic Tunnel in cooperation with NASA Ames Research Center. The purpose of the investigation was to assess the static aerodynamic characteristics of several M85 configurations in fixed-wing mode flight. These assessments will provide guidance in the future selection of M85 configuration parameters. The variables investigated were the blade sweep angle, blade chord length, shaft fairing geometry, and port-blade leading-edge orientation. Variations in the blade sweep angle will provide guidance in the selection of the number of blades for the rotary wing configuration, based on fixed-wing performance. For example, a blade sweep angle of 30° would be representative of a three-bladed configuration with the blade over the nose retracted. If the concept incorporated an advanced rotor control system, a high-fineness-ratio shaft fairing could be employed. A variation of shaft fairing geometry will provide an indication of the performance of such a fairing in the proposed configuration. A concern about the port-blade leading-edge orientation arises from the conversion process. The rotor of a helicopter manufactured in the United States rotates counterclockwise as viewed from above. Thus, after the conversion process, when a blade is over the port side, its leading edge would point aft, opposite the direction one would expect a port-wing leading edge to point. Data from such a "nonstandard" configuration will provide guidance in the selection of blade section and will also provide an indication of the need to reorient the port-blade leading edge after conversion.

Symbols

b	span of the lifting system, ft
$\bar{c}$	lifting system average chord, $\frac{S}{b}$, ft
D	drag force, lb
L	lift force, lb
M	pitching moment, ft·lb
q	free-stream dynamic pressure, $\frac{1}{2}\rho V^2$, lb/ft^2
S	lifting system planform area, ft^2
V	tunnel free-stream velocity, ft/sec
α	model angle of attack, deg
ρ	free-stream density of air, $slugs/ft^3$

Model and Apparatus

A 1/5-scale model of the XH-59A advancing blade concept helicopter was used as the baseline fuselage configuration (ref. 7). The 1/5-scale XH-59A fuselage was used only as a mounting platform for the M85 lifting system; no effort was made to scale the lifting system or to account for any discrepancies resulting from dissimilar scaling. This model was mounted on the NASA 842A six-component strain-gauge balance, which, in turn, was mounted on a sting (fig. 1). The dimensions of the model are shown in figure 2. Inclination of the model was measured by an angle-of-attack transducer mounted in the fuselage. The model did not include a horizontal tail.

The M85 configuration components consisted of two blade sets of two blades each, a hub fairing,

and two shaft fairings. The hub-fairing shape was taken from a series of shapes that were shown to have low drag characteristics (ref. 8). The blade sets were aluminum, with RC(3)-10 airfoil sections (ref. 9). This airfoil section was chosen because it is representative of an advanced rotor blade airfoil. A sketch of both blades is shown in figure 3. One set had a chord length of 4.5 inches and was designated the narrow-chord blade set. The other set had a chord length of 6.75 inches and was designated the wide-chord blade set. The hub fairing was designated the H300. The cross section and geometric properties of the H300 are shown in figure 4. The two shaft fairings were designated the S40 and the S300. Their cross sections and geometric properties are shown in figure 5. The thickness ratio of the S40 was 0.34; the thickness ratio of the S300 was 0.15.

Test Procedures and Conditions

Angle-of-attack sweeps that ranged from $-2°$ to $10°$ (in $2°$ increments) were made during each test run. These sweeps were made to assess the aerodynamic effects of various M85 configuration parameters. A photograph of a typical M85 configuration is shown in figure 6. The configuration parameters that were varied during the test were blade sweep angle, blade chord length, and shaft fairing geometry. The blade sweep angles were $0°$, $30°$, and $45°$; the blade chord was varied by changing the blade set; the shaft fairing geometry was varied by interchanging the S40 and the S300. One run was made with the port-blade leading edge downstream. Runs were also made that did not include all the model components: Runs were made with the shaft fairing removed (the hub fairing was mounted flush to the top of the fuselage model), and one run was made with no blades mounted on the hub fairing. A test matrix that correlates each run number with a run configuration is shown in table I. Weight tare runs were also made for each major model configuration change.

All test data runs were conducted at low speed with a dynamic pressure of 80 pounds per square foot. The test section was fully closed, and the free-stream Reynolds number was approximately 1 500 000 per foot.

Force and moment, angle-of-attack, and test section conditions data were acquired by a Hewlett Packard 2250 Data Acquisition Unit (DAU). The DAU data were reduced by a MODCOMP Classic computer with the data sample rate set at 40 samples per point. Weight tare corrections and transformations from balance axes to wind axes were applied to the data by the computer. All moment data were referenced to the point shown in figure 2.

Data Accuracy

No corrections were applied to the data. Model blockage at the maximum α was 0.86 percent of the test section area. The model was unpowered, and the largest lifting surface span was only 36 percent of the test section span. Sting interference tares were not made. Sting-on-fuselage interference drag and model cavity pressure drag were neglected; however, note that these drag forces do have a significant effect on overall configuration drag levels and thus on lift-to-drag ratios.

The documented accuracy of Langley Research Center internal strain-gauge balances is 0.5 percent of the maximum beam load for each component. The accuracy figures for all six components of the 842A balance were translated into engineering units and are listed in table II. Note that, in practice, data repeatabilities of 0.1 percent to 0.2 percent have been achieved.

Data Presentation

No fuselage tares were removed from the data; that is, each configuration includes the fuselage. The data were reduced to the rotorcraft industry standard of forces and moments divided by dynamic pressure. This is a common practice throughout the rotorcraft industry. The reference areas and lengths from each configuration that would be used to reduce the data to standard coefficients are listed in table III. Data were compared to a baseline model configuration shown in figure 7. Data comparison figures referenced in the discussion of results are listed in the following table:

	Figure
Effect of blade sweep	8
Effect of blade chord width	9
Effect of shaft fairing geometry	10
Effect of port-blade leading-edge orientation	11
Aerodynamic characteristics of a blades-off configuration	12

Also, all data are presented in the appendix (figs. A1–A18) by run number as plots of $D/q, L/q$ and M/q versus α, and D/q versus L/q. The slopes of the L/q and M/q versus α curves were extracted from least-squares curve fits of the data and are tabulated by run number in table IV. The maximum lift-to-drag ratios are also included in table IV. These ratios reflect the lifting efficiency of each configuration.

Results and Discussion

Because of the disproportionate scaling between the fuselage and lifting system models, conclusions drawn from this investigation are qualitative. The baseline configuration consisted of the wide-chord blades set at a sweep angle of 0° on the H300 hub fairing, which, in turn, was mounted on the S300 shaft fairing. The S300 was mounted on the fuselage model.

The discussion will focus on the effect each configuration parameter had on the aerodynamic characteristics of the lifting systems. In general, the data presented in this report correlated favorably with similar data presented in reference 10.

Effect of Blade Sweep

A comparison of data from the baseline (blade sweep angle of 0°) and the two wide-chord, swept-blades configurations is shown in figure 8. Aside from the difference in blade sweep angle, all other configuration parameters were the same. As expected, L/q versus α slopes were proportional to the cosine of the blade sweep angle. The configuration that had a sweep angle of 30° displayed a lower L/q versus α slope and a reduction in maximum lift-to-drag ratio when compared to the baseline configuration. In a similar comparison, the configuration with a sweep angle of 45° also showed a decrease in both L/q versus α slope and maximum lift-to-drag ratio. The configuration with a sweep angle of 30° had a less positive M/q versus α slope compared to the baseline, as did the configuration with a sweep angle of 45°. A trim analysis of the data indicated that the addition of a horizontal tail would not qualitatively alter the comparisons of the lift and drag data. This addition would obviate any stability concerns. These results imply that the baseline configuration offers more lift, with greater efficiency, than either of the other configurations.

Effect of Blade Chord Length

A comparison of data between the baseline configuration (wide chord) and the narrow-chord blades configuration is shown in figure 9. Aside from the difference in chord length, all other configuration parameters were the same. The purpose of this aspect of the test was to assess the effect of an increase in blade chord, thus blade area, with no change in other lifting system parameters. The data show that the baseline configuration displayed more favorable lift and similar drag characteristics when compared to the narrow-chord configuration with a sweep angle of 0°. However, as the sweep angle increased, the lifting advantage of the wide-chord configuration decreased. At a sweep angle of 45°, the L/q and D/q versus α curves were the same for both configurations. The apparent disagreement of the results with classical theory could be attributed to a more favorable interaction of the wide-chord blades compared with the narrow-chord blades, with the wake shed from the disk lateral edge. A scrutiny of a very limited amount of tuft photography taken in the test tends to support this hypothesis. Slightly lower M/q versus α slopes were also obtained for the wide-chord configurations. These results imply that a wider chord blade configuration would be a better choice for design. However, owing to the interactional nature of the wide-chord advantage, it is recommended that these configurations be investigated further to identify the aerodynamic mechanisms involved.

Effect of Shaft Fairing Geometry

A comparison of data from the baseline (S300) configuration and from an alternate shaft fairing (S40) configuration is shown in figure 10. Aside from the difference in shaft fairings, all other parameters were the same. The D/q versus α plot suggests that the drag for both configurations was similar. However, the L/q values of the S40 configuration were lower than those of the baseline configuration, with a correspondingly lower maximum lift-to-drag ratio. The M/q values were also higher for the S40 configuration. These results imply that the baseline fairing is more efficient than the more conventional S40 fairing. The baseline fairing also contributes more favorably to aircraft stability. The M85 concept could benefit from rotor control system designs that would allow the use of high-fineness-ratio shaft fairings such as the S300.

Effect of Port-Blade Leading-Edge Orientation

A comparison of data from the two blade leading-edge orientations is shown in figure 11. The rotary wing configuration had the port-blade leading edge pointed in the downstream direction. The fixed-wing configuration, in contrast, had the port-blade leading edge pointing in the upstream direction. Both configurations had narrow-chord blades set at a sweep angle of 30°. The data suggest no significant differences existed between the overall aerodynamic characteristics of the two configurations. However, the port-blade leading-edge orientation was varied for one configuration only, and the angle of attack did not approach a value at which the blade stalled. Therefore, in light of the limited amount of data, neither configuration could be termed the "best." Since port-blade leading-edge orientation can have a significant effect on both high angle of attack and helicopter-mode flight, further investigation of the effect of this parameter is warranted.

Blades-Off Characteristics

A comparison of data from a bladeless configuration with data from the baseline configuration is shown in figure 12. Except for blades on the baseline configuration, both configurations were identical. The data show that, as expected, the bladeless configuration lift curve slope was significantly lower than that of the baseline configuration. In comparison, the D/q values obtained for both configurations were very similar throughout the α range. The values were nearly identical between 0° and 2.5°. These results, along with the D/q versus L/q plot and maximum lift-to-drag ratio, suggest that the lifting efficiency of the baseline configuration is comparatively very good, whereas that of the bladeless configuration is relatively low. These results also suggest that further study of the conversion flight regime is warranted to determine the effect of this lower efficiency on the overall flight profile.

Conclusions

An experimental investigation of the fixed-wing mode aerodynamic characteristics of a stoppable rotor-wing hybrid aircraft design was conducted in the Langley 14- by 22-Foot Subsonic Tunnel. The following conclusions were drawn from analysis of the data obtained:

1. The configuration with a blade sweep angle of 0° resulted in the most favorable aerodynamic characteristics. This choice would allow maximum flexibility in the selection of the number of blades for the helicopter mode configuration.
2. Wide-chord blades would result in better disk-wing aerodynamic characteristics when compared to narrow-chord blades of the same airfoil section. However, owing to the interactional nature of the advantage of the wide-chord blades, it is recommended that these configurations be investigated further to identify the aerodynamic mechanisms involved.
3. For the M85 configuration, the use of a high-fineness-ratio shaft fairing resulted in better aerodynamic characteristics. The M85 concept could benefit from rotor control system designs that would allow the use of this type of fairing, as opposed to more conventional shaft fairings.
4. For the configurations tested, no significant differences were found between the aerodynamic characteristics of the two port-blade leading-edge orientations. The limited nature of the data warrants further investigation of the effect of this parameter.
5. The results suggest a need for further study of the conversion flight regime in order to fully assess the effects of the bladeless configuration on the overall flight profile.

NASA Langley Research Center
Hampton, VA 23665-5225
February 1, 1991

Appendix

Data Plots

This appendix contains plots of aerodynamic data arranged in order of increasing run number. See figures A1–A18. The following kinds of plots are presented in each figure:

D/q versus α

L/q versus α

M/q versus α

D/q versus L/q

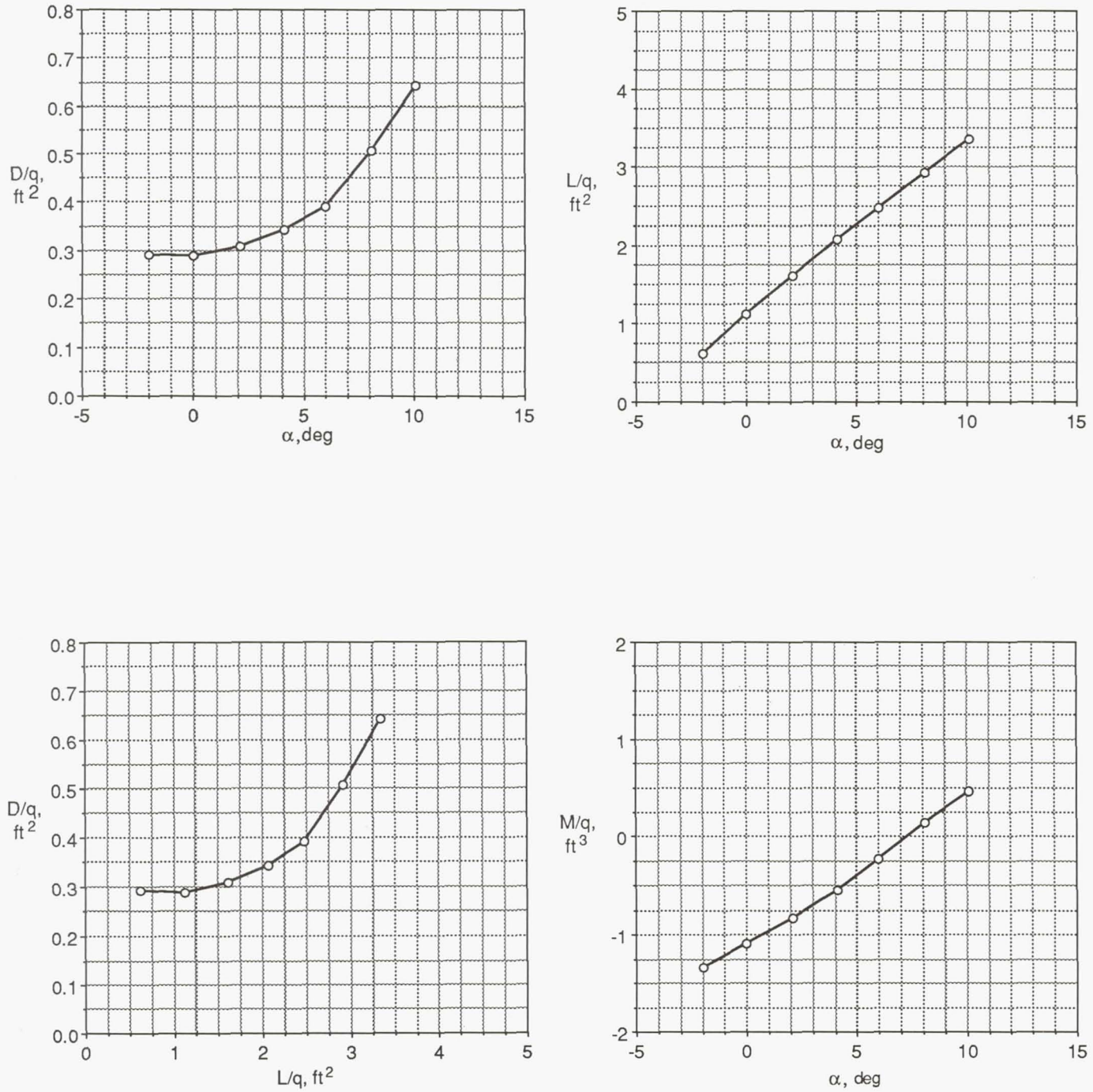

Figure A1. Aerodynamic characteristics of an M85 configuration consisting of narrow-chord blades at a sweep angle of 30° with no shaft fairing (run 402).

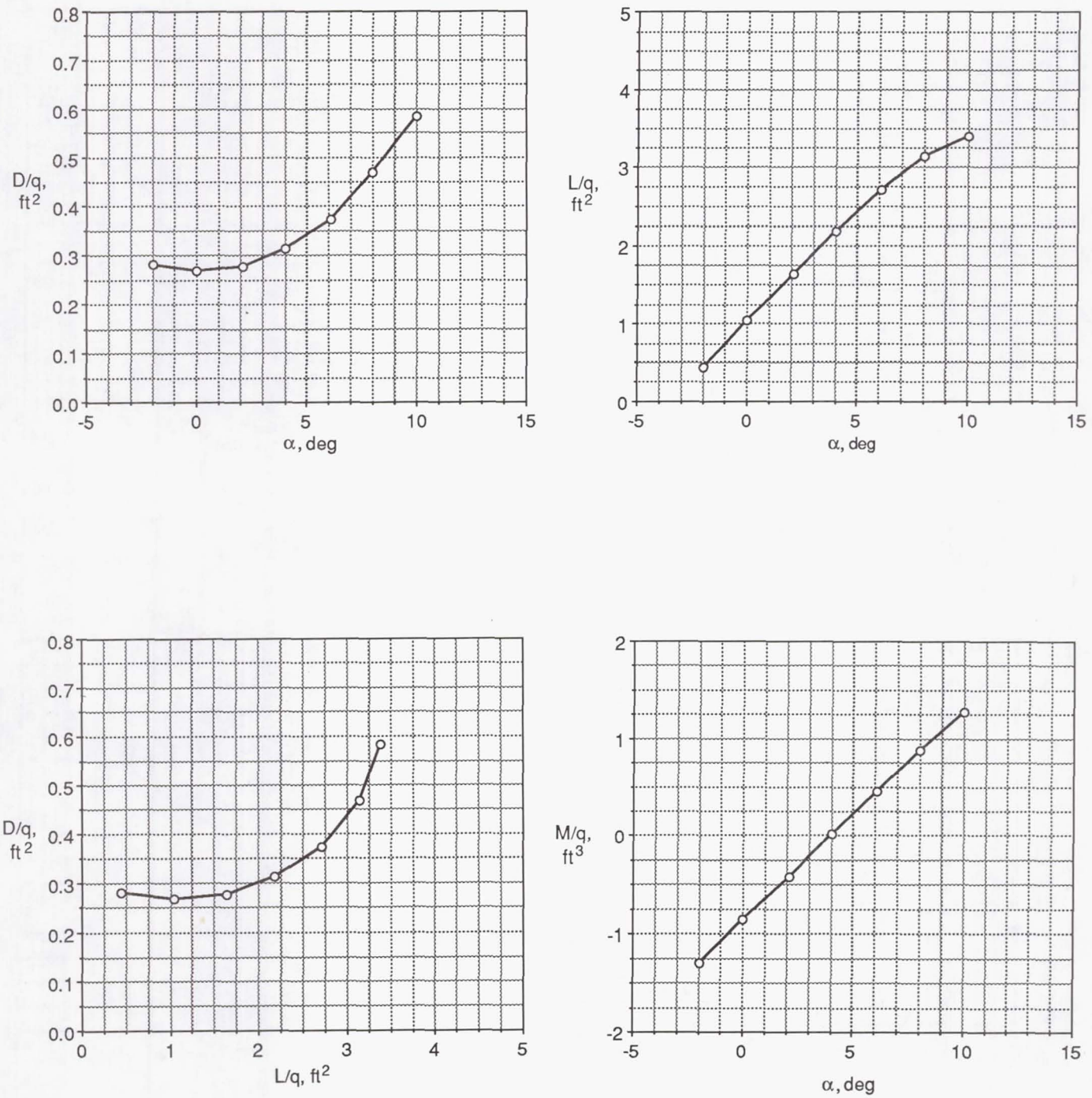

Figure A2. Aerodynamic characteristics of an M85 configuration consisting of narrow-chord blades at a sweep angle of 0° with no shaft fairing (run 403).

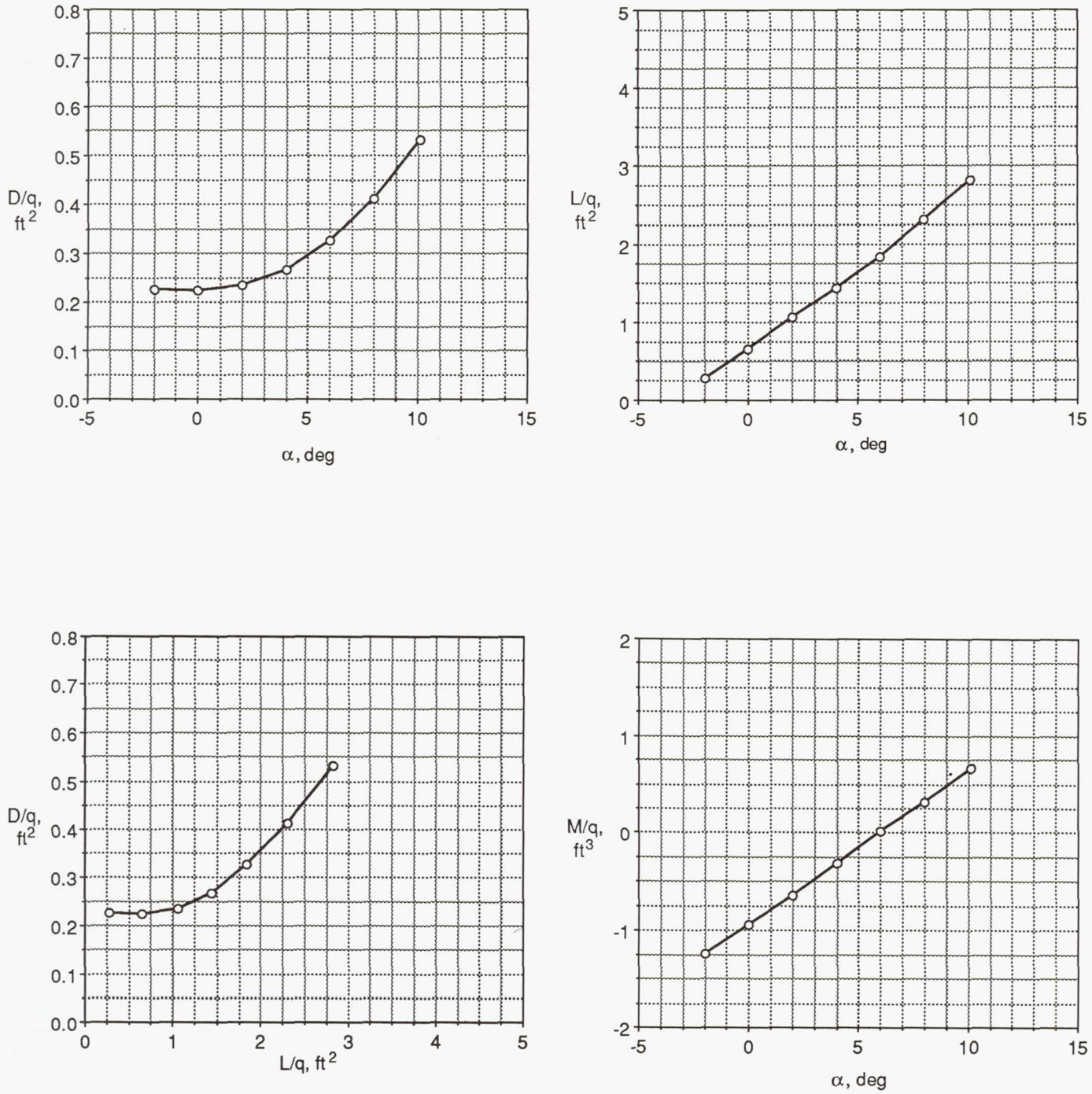

Figure A3. Aerodynamic characteristics of an M85 configuration consisting of narrow-chord blades at a sweep angle of 45° with the hub mounted on the S300 shaft fairing (run 406).

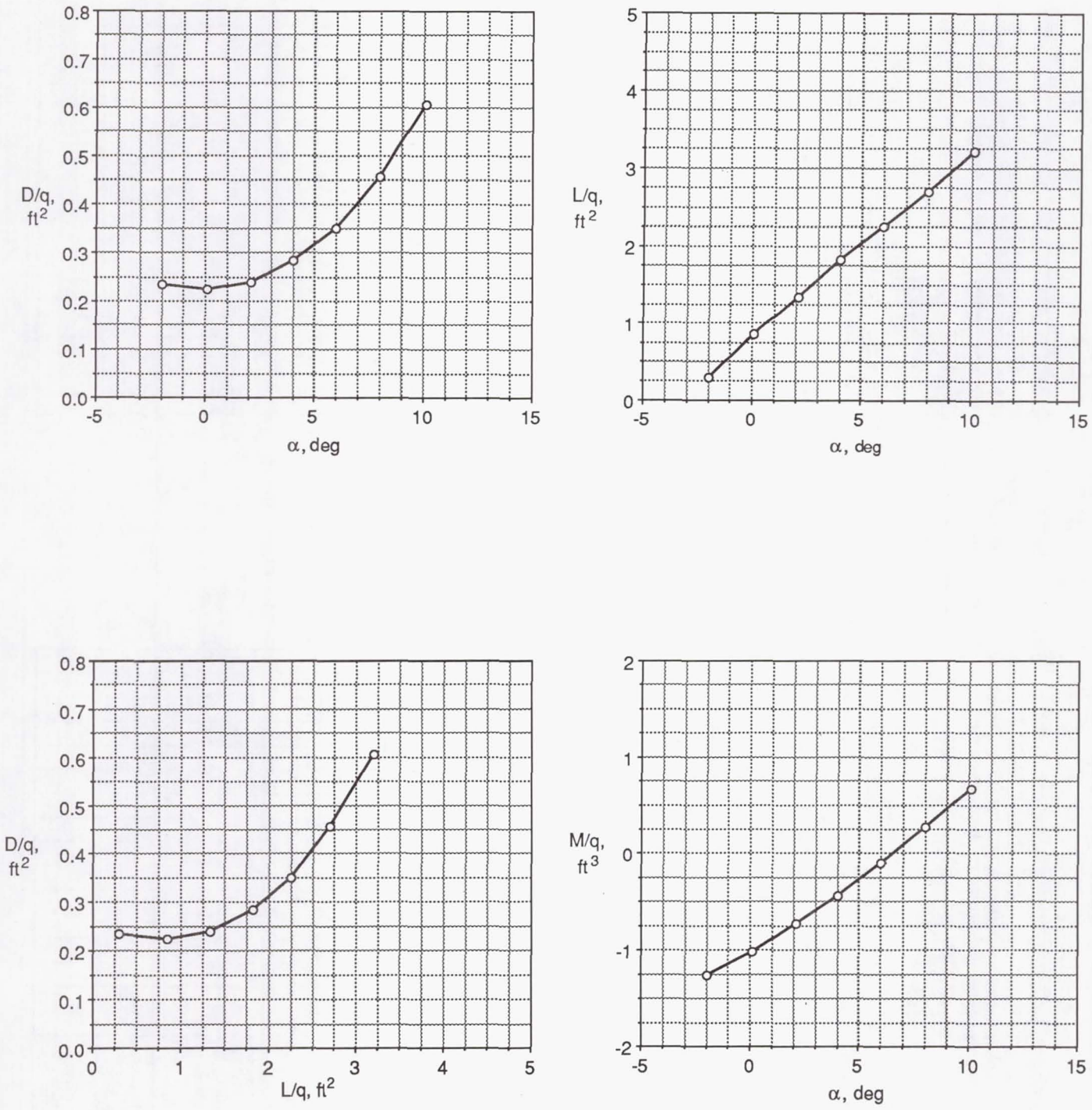

Figure A4. Aerodynamic characteristics of an M85 configuration consisting of narrow-chord blades at a sweep angle of 30° with the port-blade leading edge pointed downstream and the hub mounted on the S300 shaft fairing (run 407).

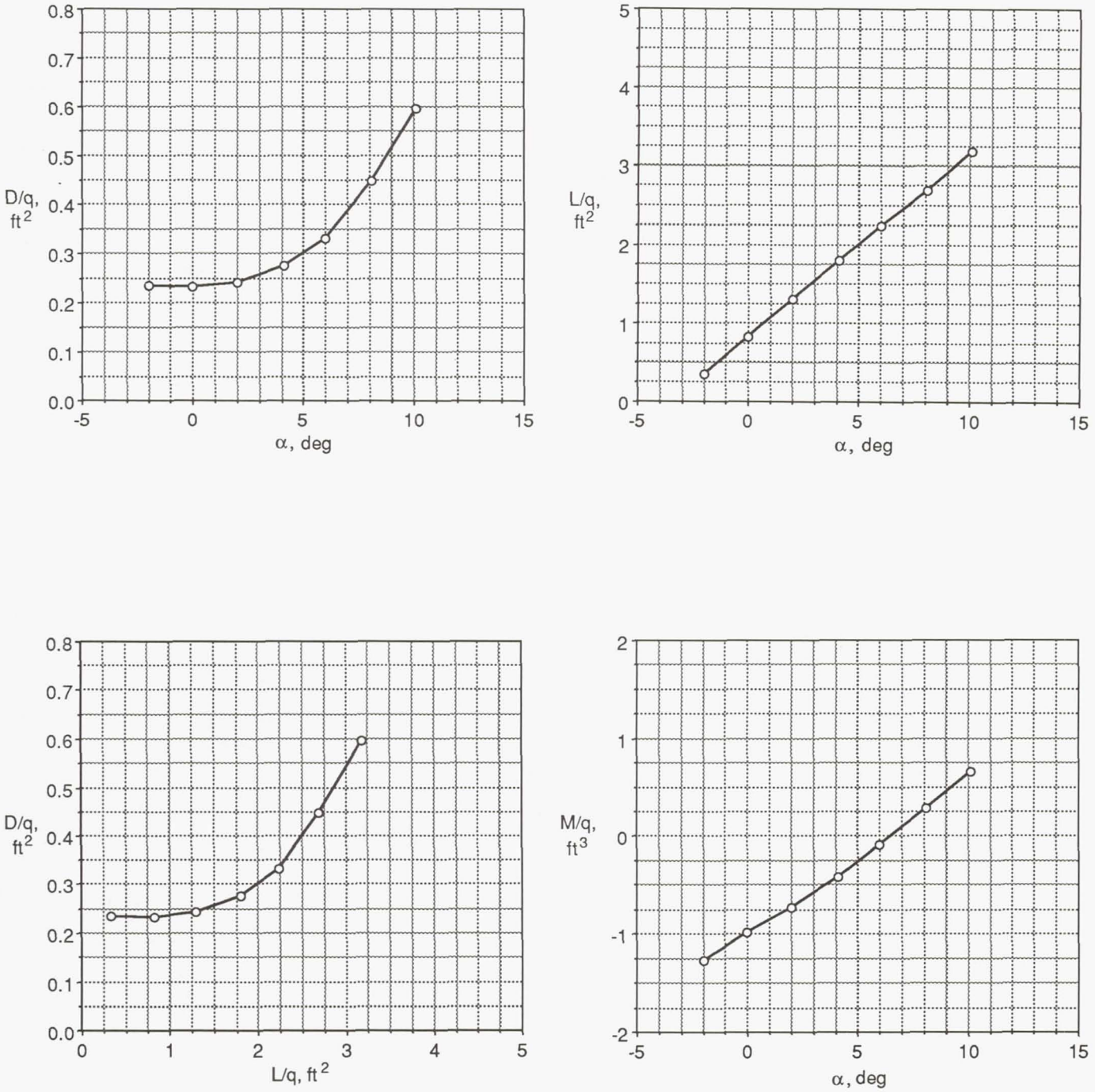

Figure A5. Aerodynamic characteristics of an M85 configuration consisting of narrow-chord blades at a sweep angle of 30° with the hub mounted on the S300 shaft fairing (run 409).

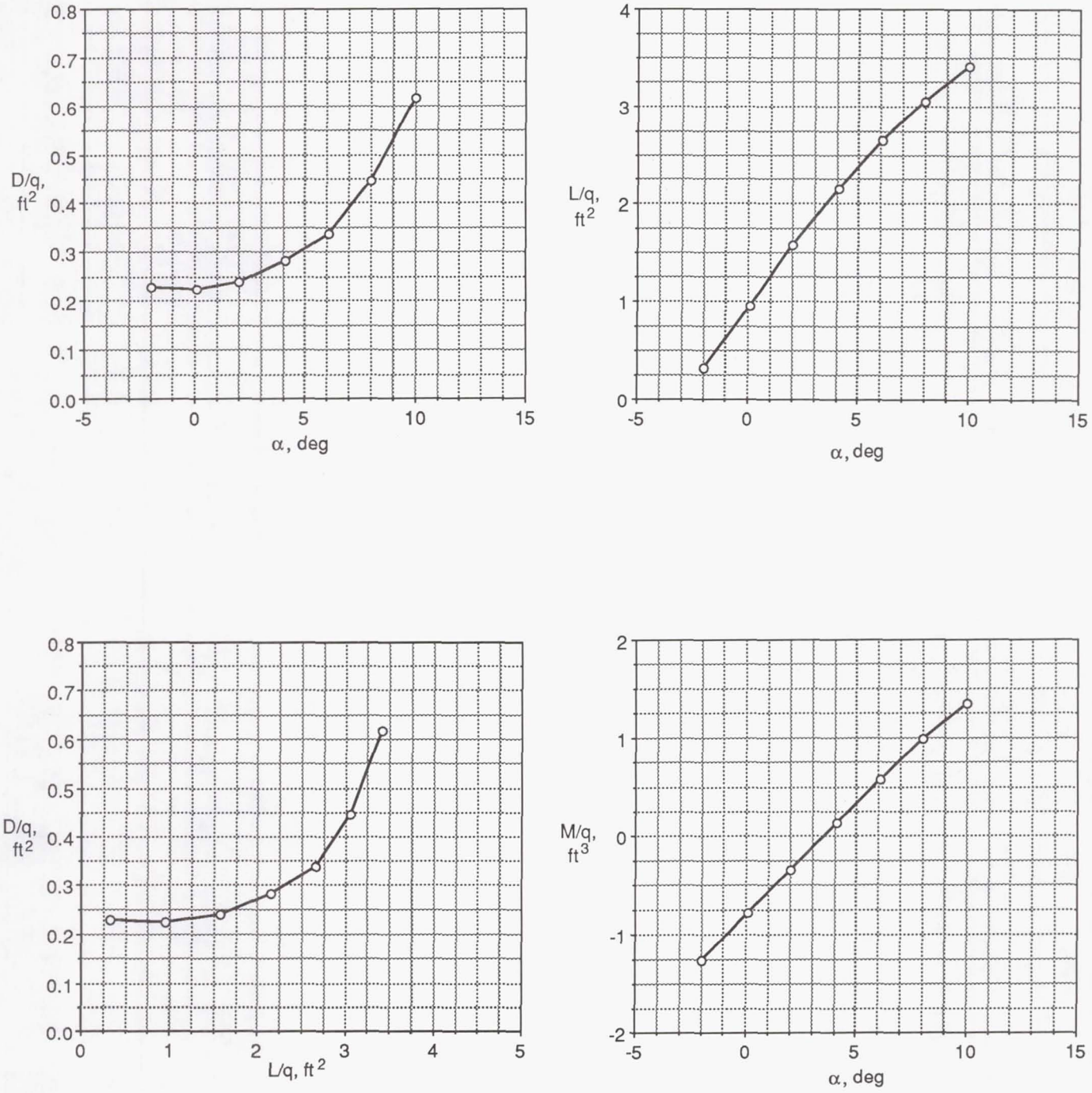

Figure A6. Aerodynamic characteristics of an M85 configuration consisting of narrow-chord blades at a sweep angle of 0° with the hub mounted on the S300 shaft fairing (run 410).

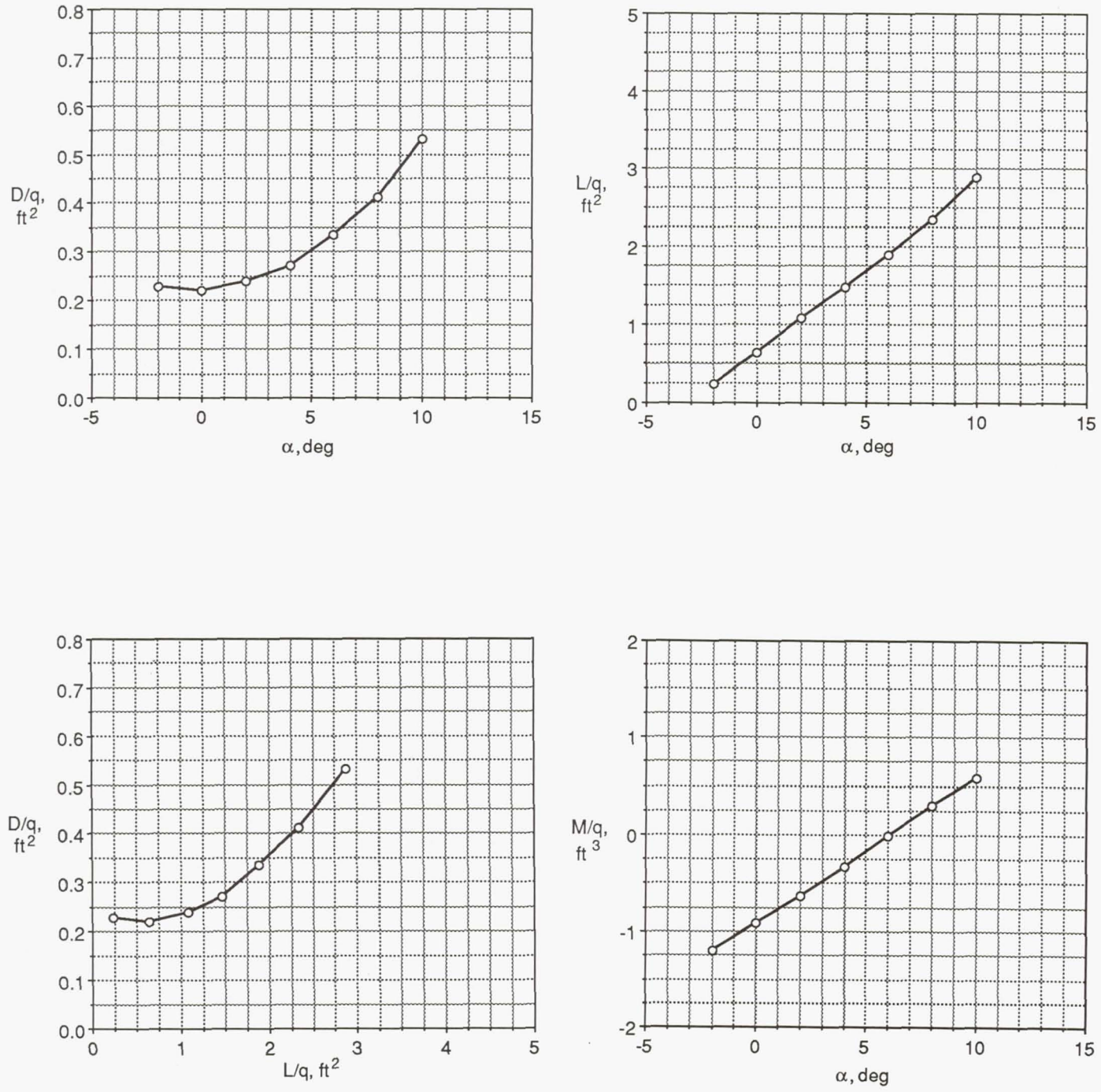

Figure A7. Aerodynamic characteristics of an M85 configuration consisting of wide-chord blades at a sweep angle of 45° with the hub mounted on the S300 shaft fairing (run 411).

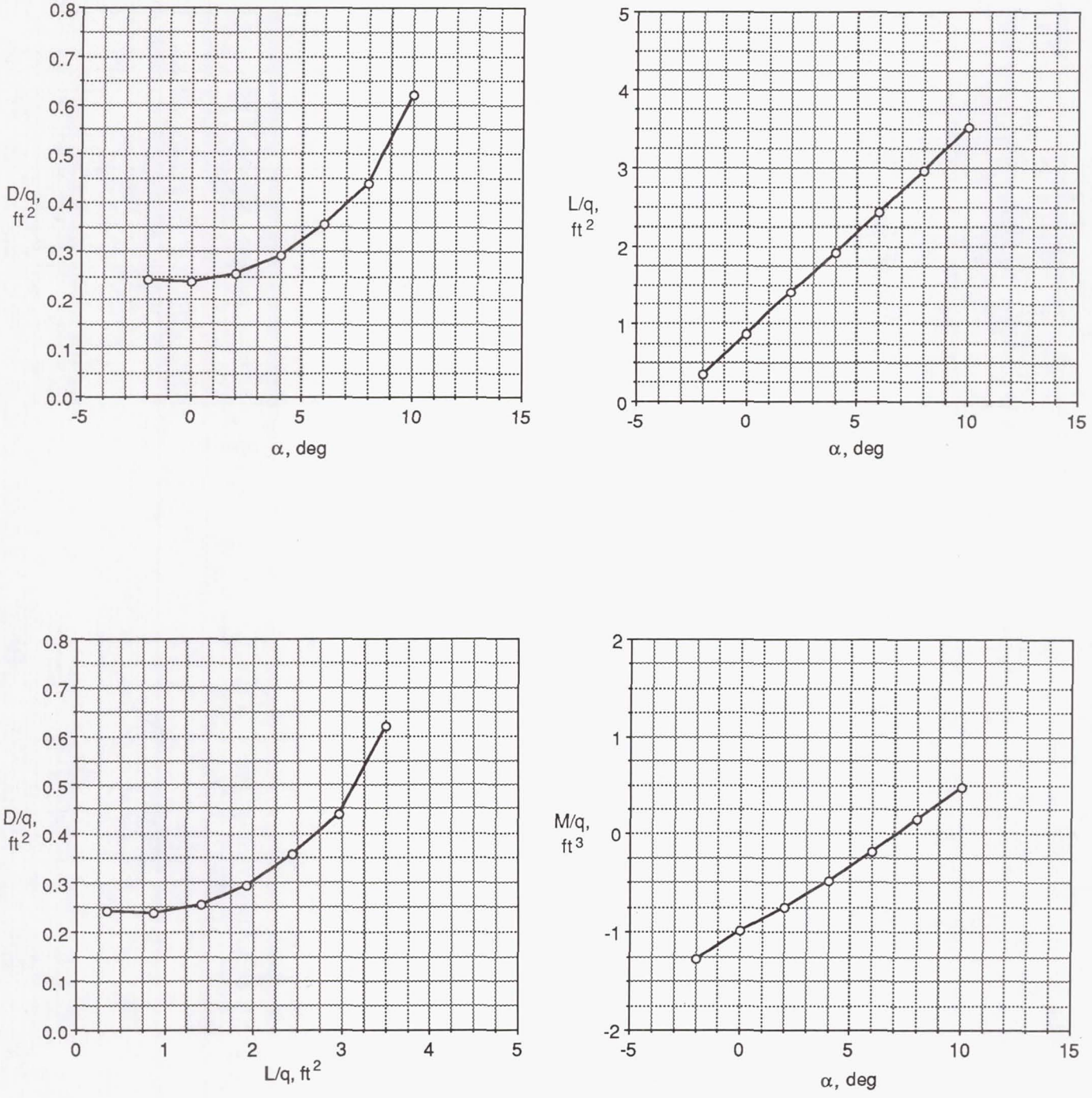

Figure A8. Aerodynamic characteristics of an M85 configuration consisting of wide-chord blades at a sweep angle of 30° with the hub mounted on the S300 shaft fairing (run 412).

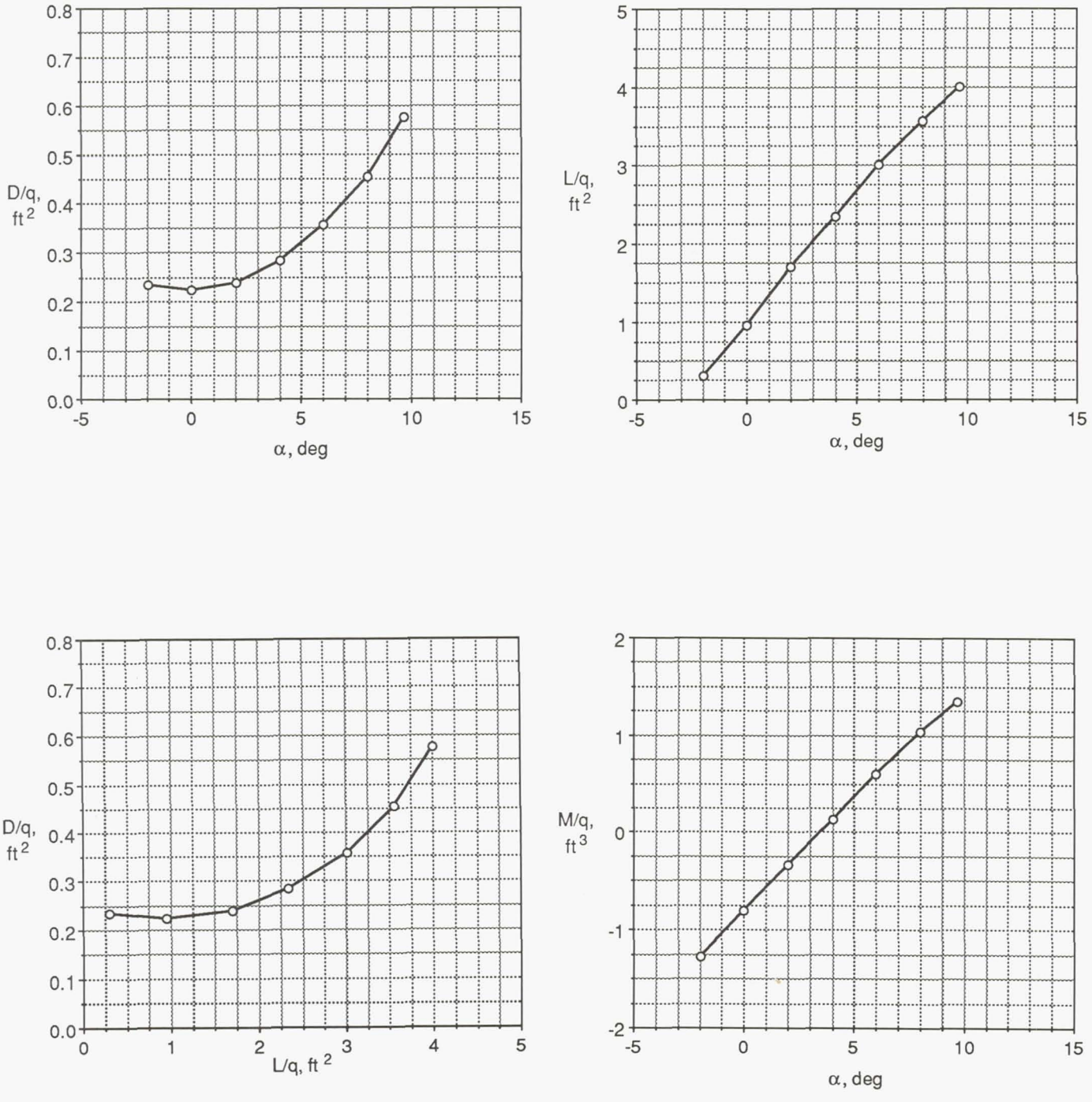

Figure A9. Aerodynamic characteristics of the baseline M85 configuration consisting of wide-chord blades at a sweep angle of 0° with the hub mounted on the S300 shaft fairing (run 413).

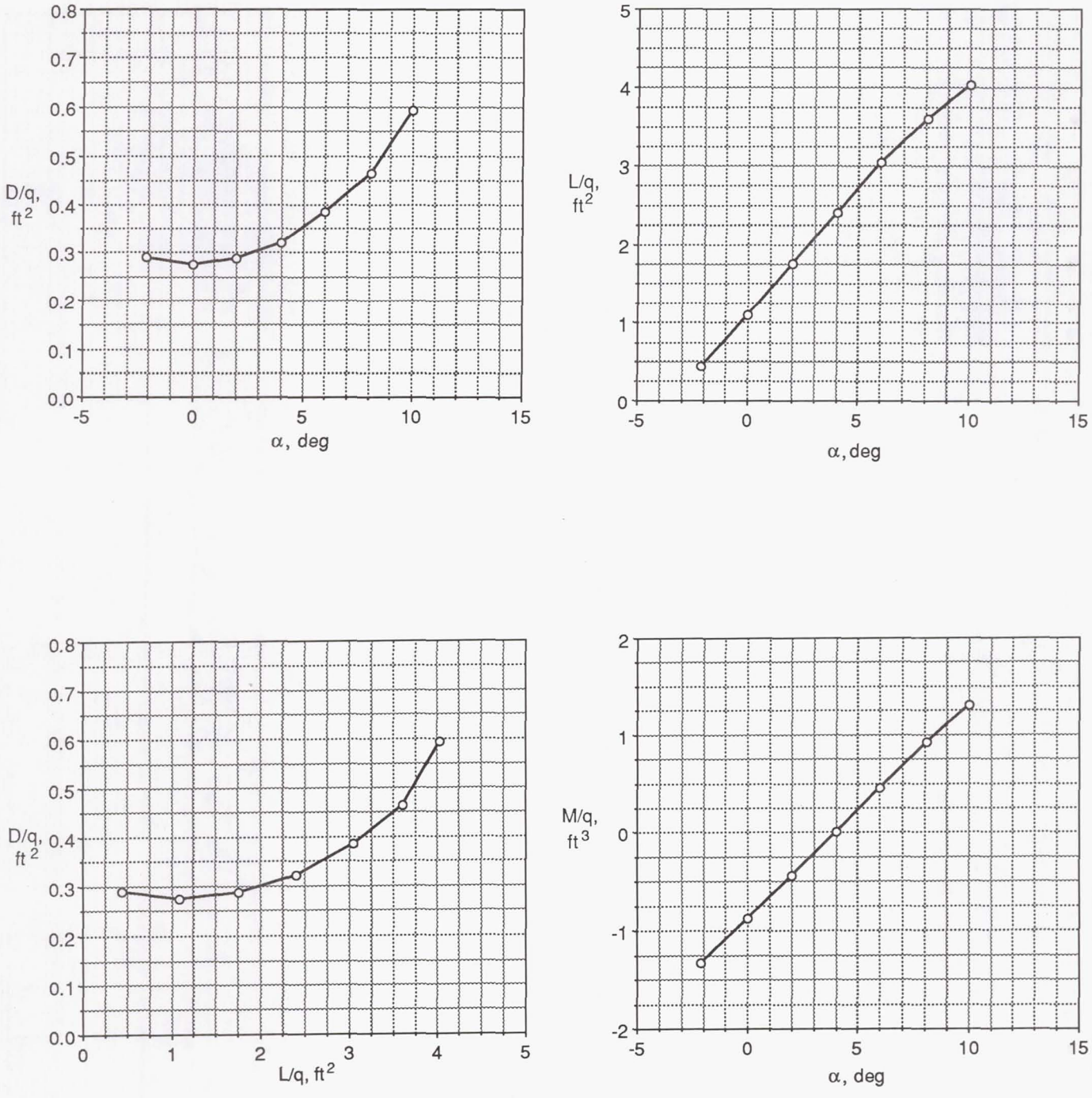

Figure A10. Aerodynamic characteristics of an M85 configuration consisting of wide-chord blades at a sweep angle of 0° with no shaft fairing (run 414).

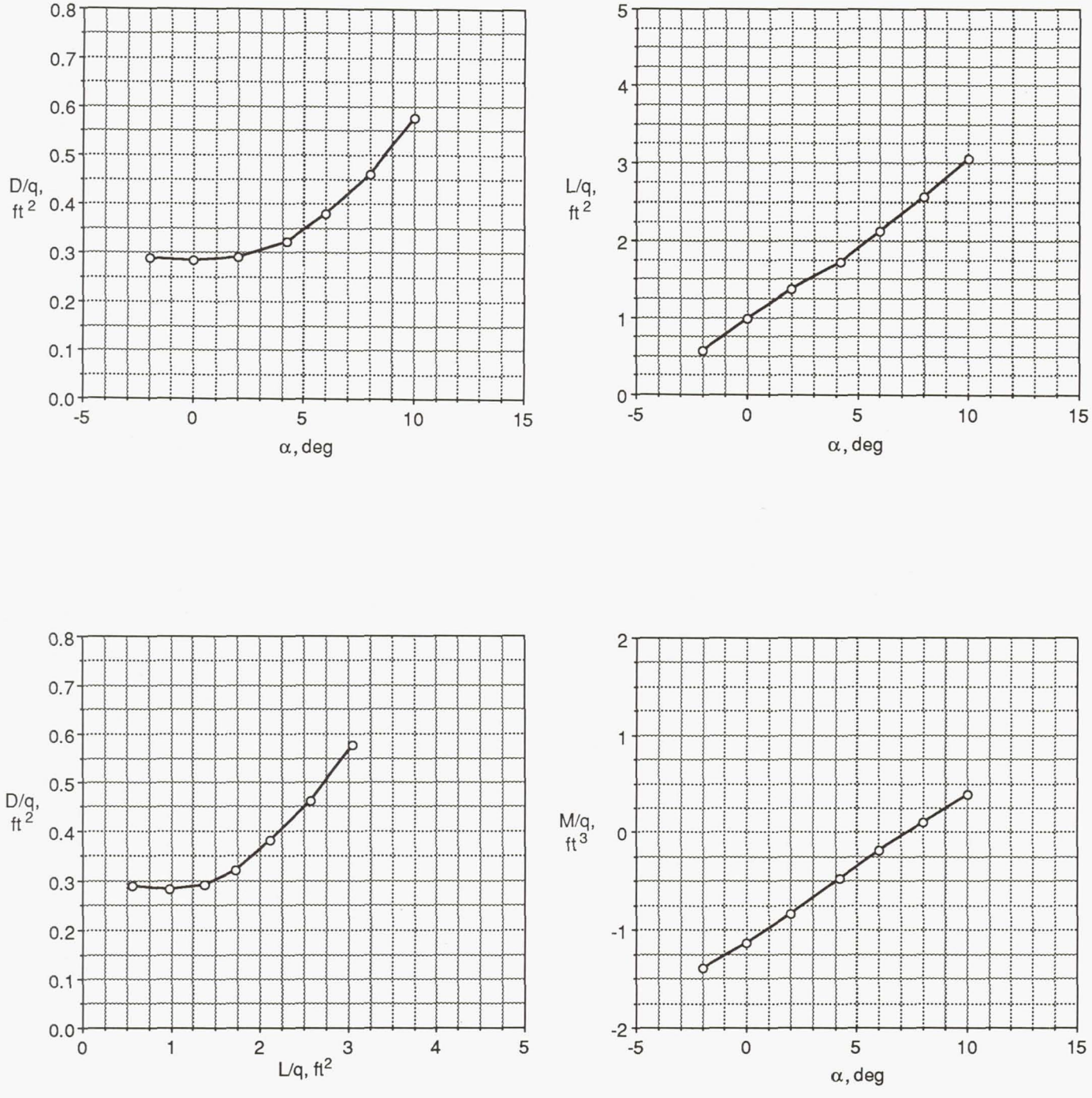

Figure A11. Aerodynamic characteristics of an M85 configuration consisting of wide-chord blades at a sweep angle of 45° with no shaft fairing (run 415).

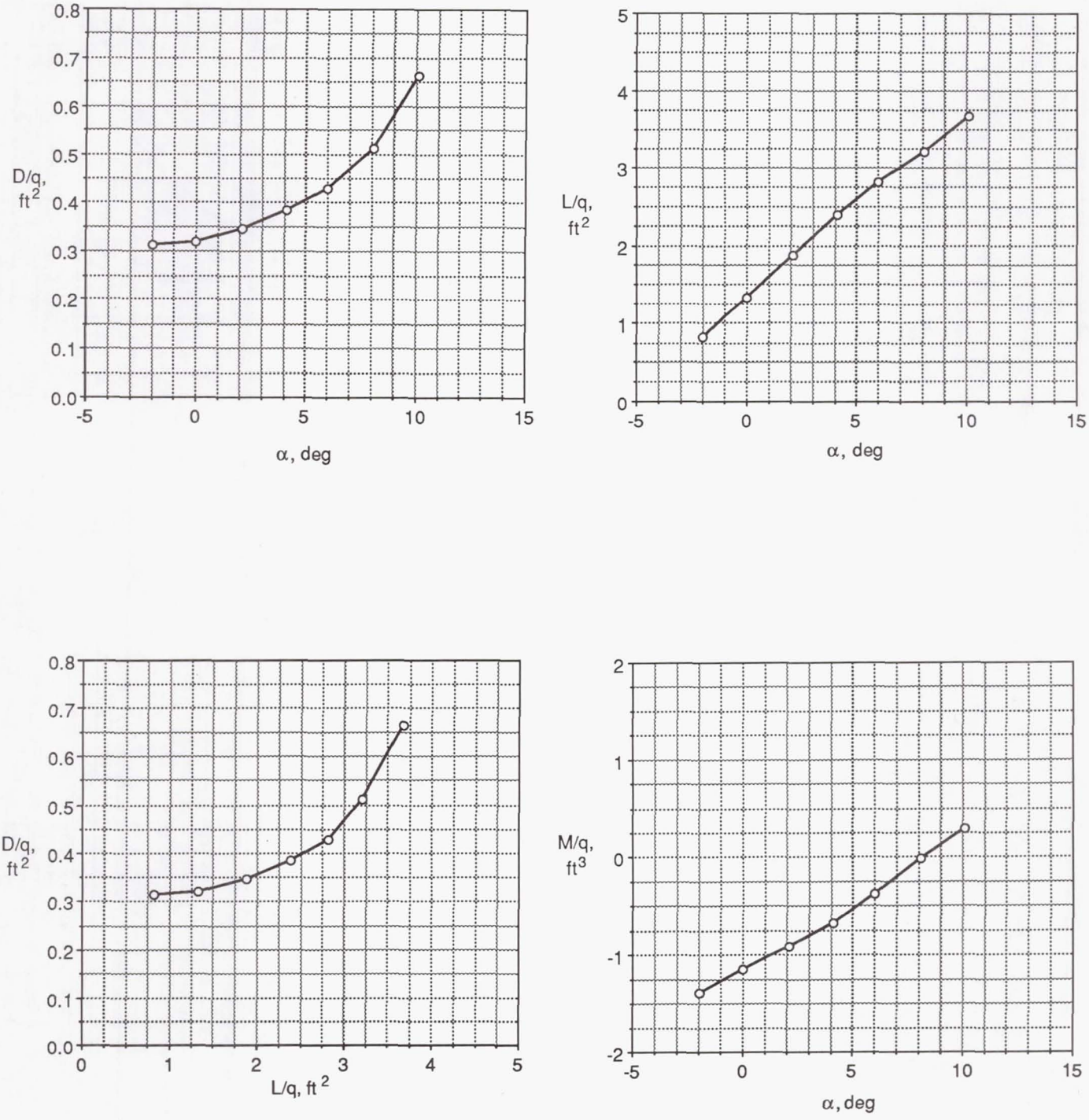

Figure A12. Aerodynamic characteristics of an M85 configuration consisting of wide-chord blades at a sweep angle of 30° with no shaft fairing (run 416).

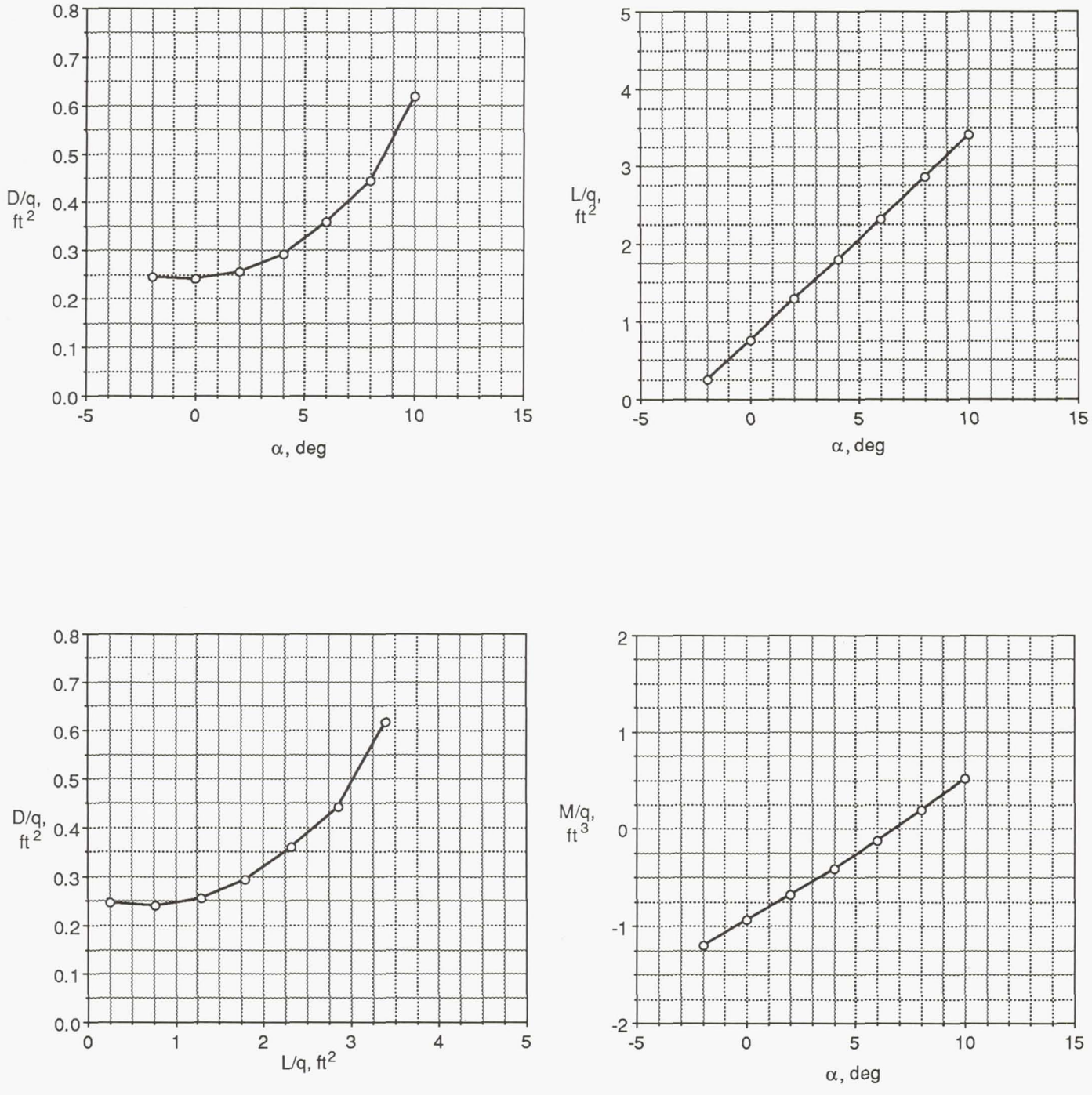

Figure A13. Aerodynamic characteristics of an M85 configuration consisting of wide-chord blades at a sweep angle of 30° with the hub mounted on the S40 shaft fairing (run 417).

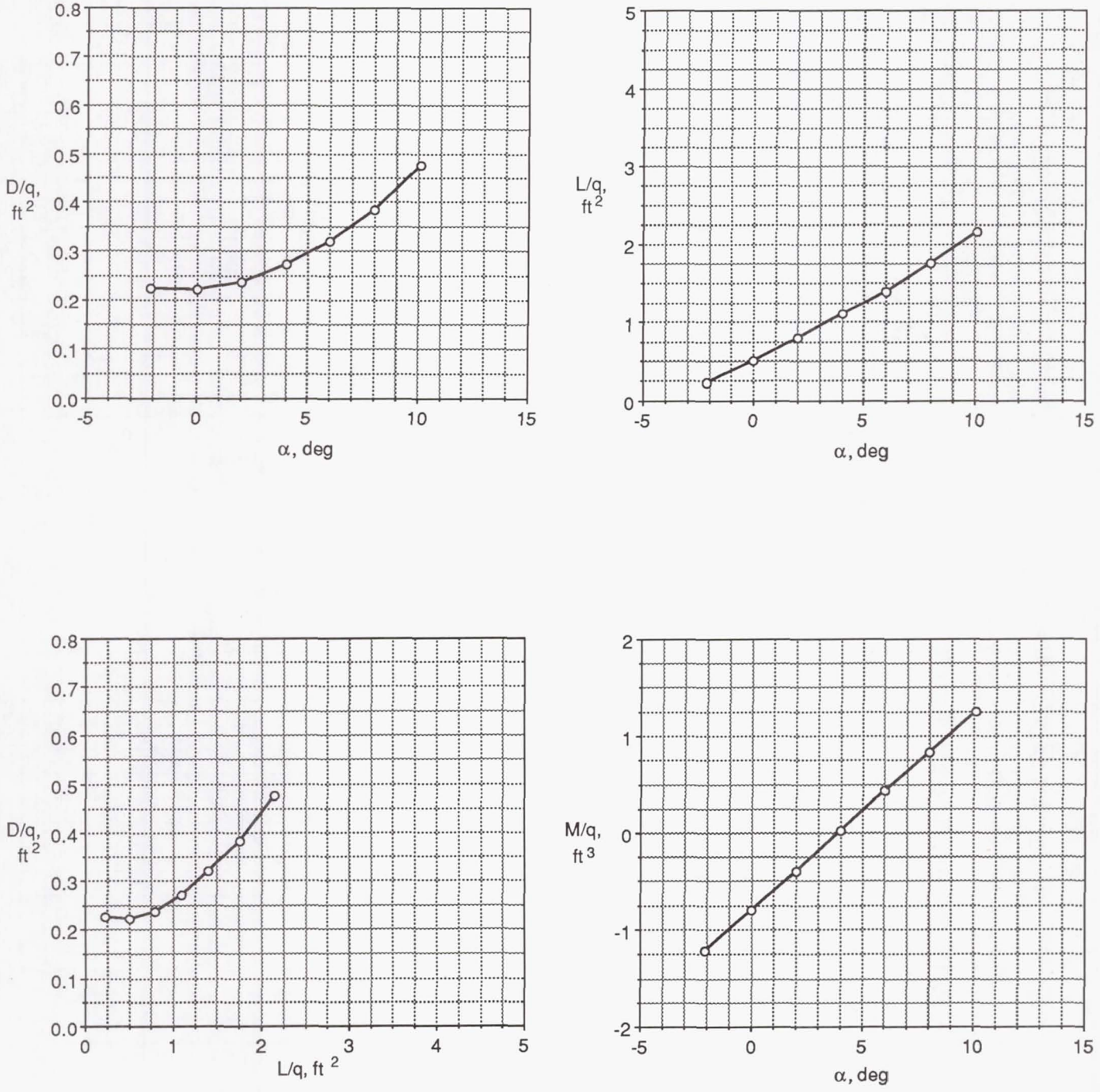

Figure A14. Aerodynamic characteristics of an M85 configuration consisting of the hub alone mounted on the S40 shaft fairing (run 420).

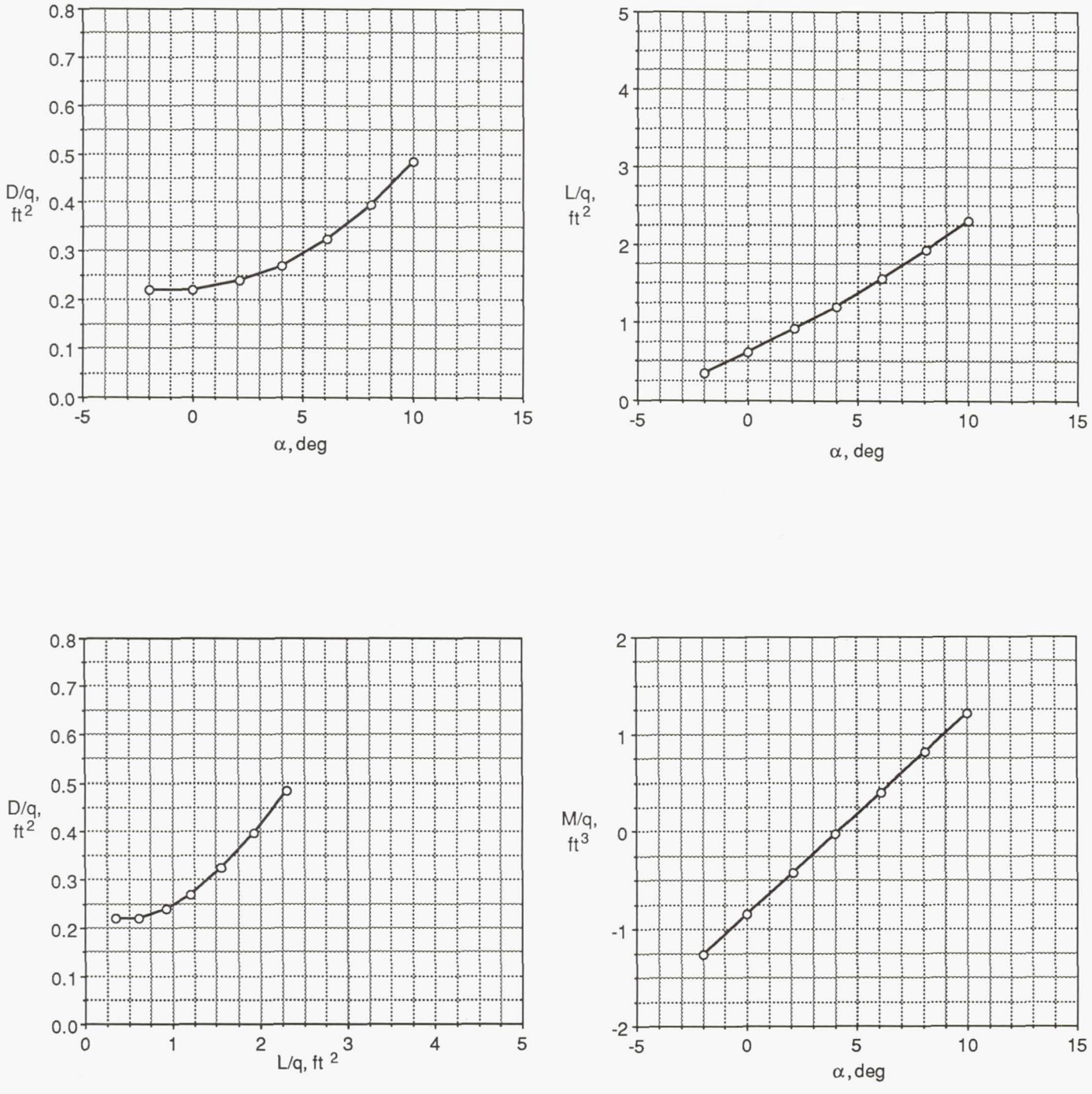

Figure A15. Aerodynamic characteristics of an M85 configuration consisting of the hub alone mounted on the S300 shaft fairing (run 421).

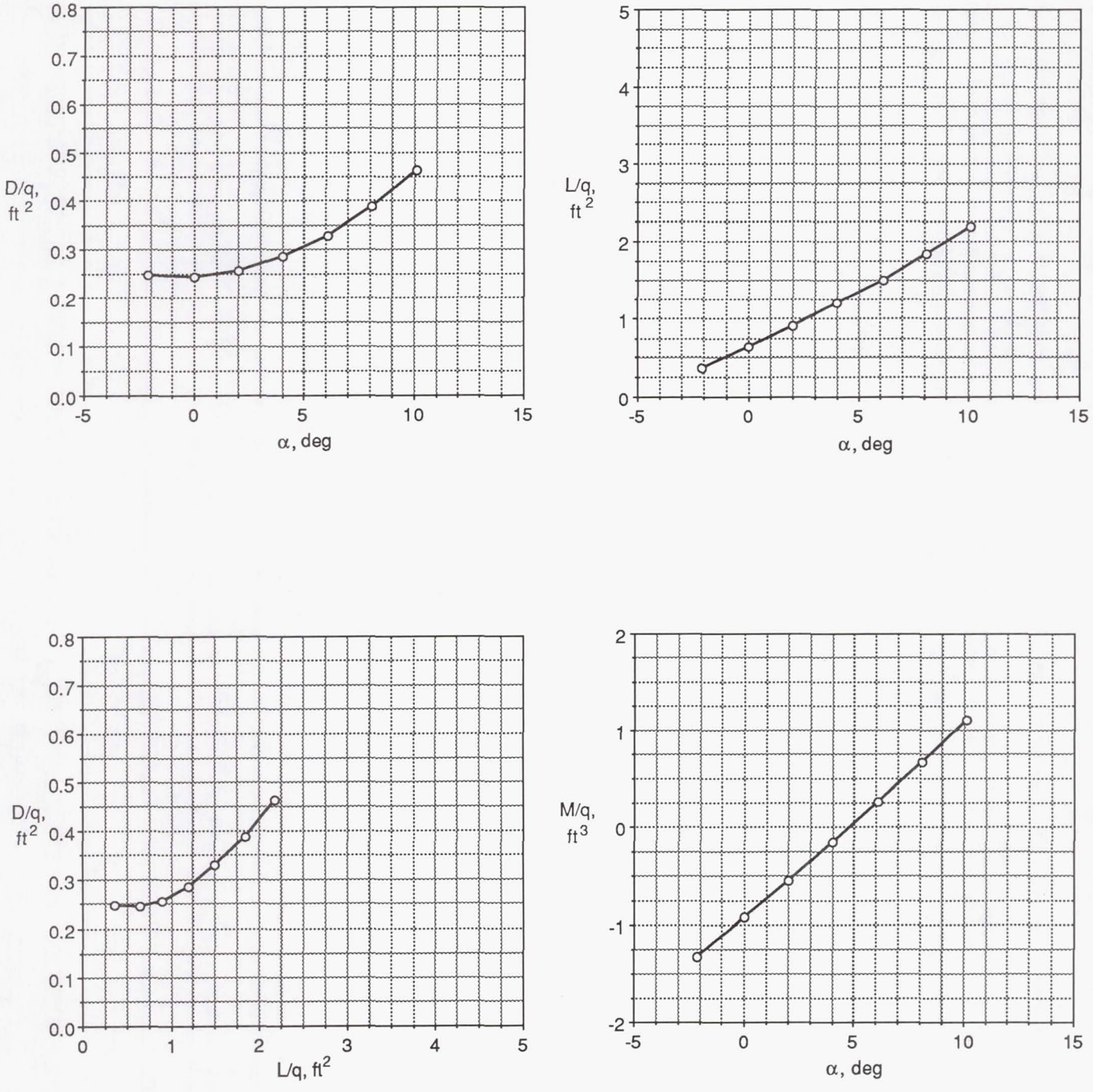

Figure A16. Aerodynamic characteristics of an M85 configuration consisting of the hub alone mounted flush to the fuselage (run 422).

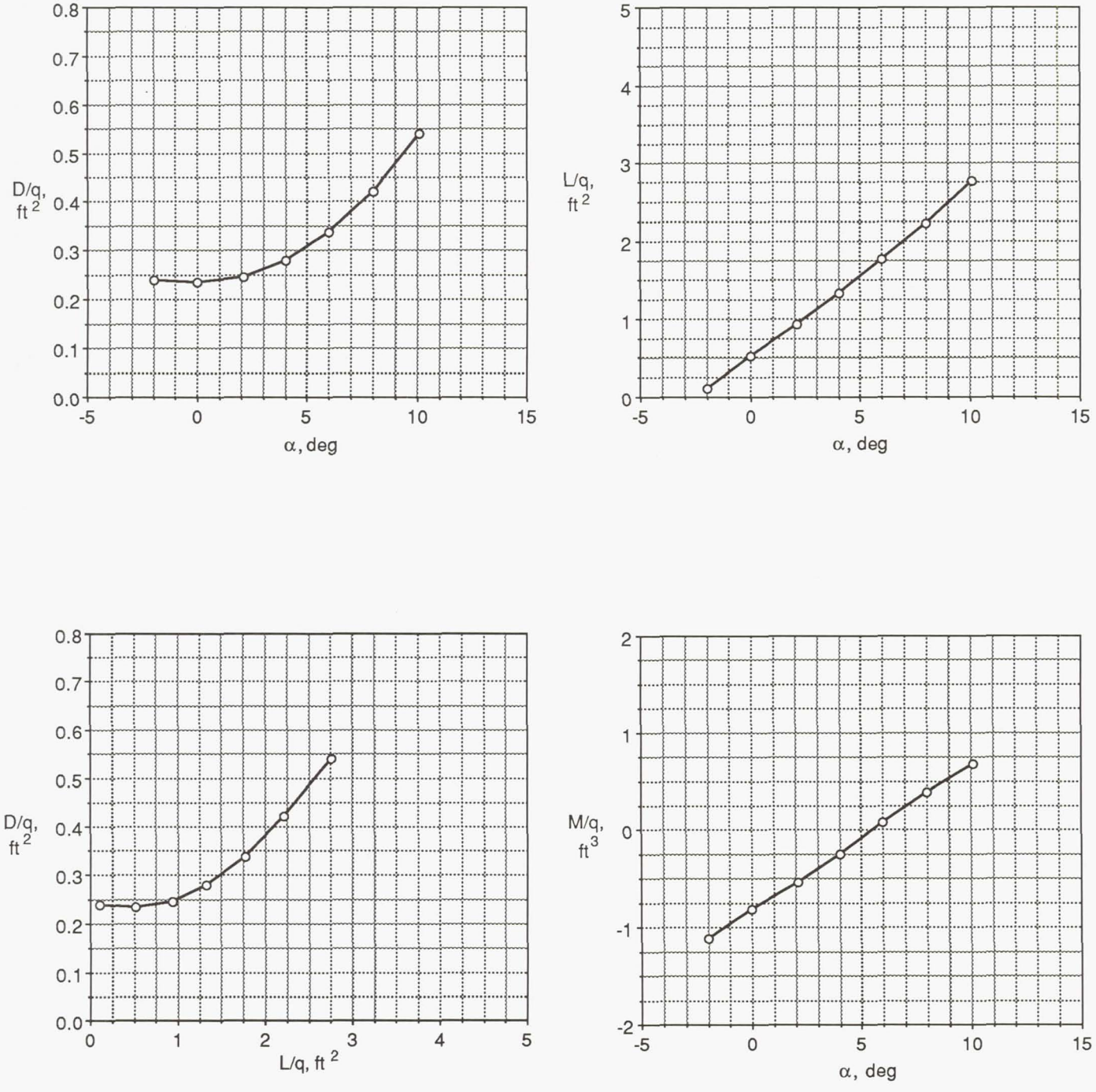

Figure A17. Aerodynamic characteristics of an M85 configuration consisting of wide-chord blades at a sweep angle of 45° with the hub mounted on the S40 shaft fairing (run 423).

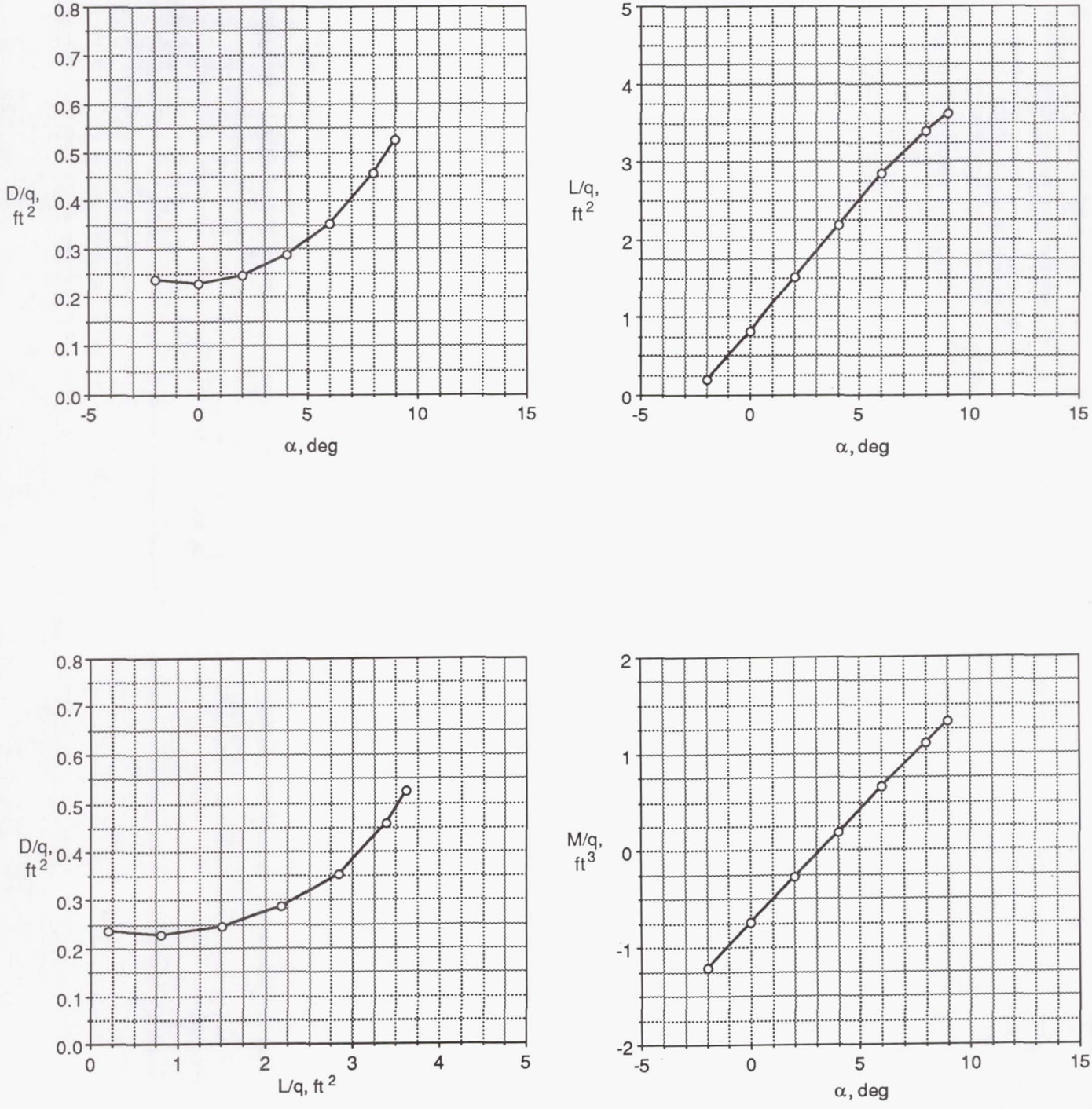

Figure A18. Aerodynamic characteristics of an M85 configuration consisting of wide-chord blades at a sweep angle of 0° with the hub mounted on the S40 shaft fairing (run 424).

References

1. Reeder, John P.: *Handling Qualities Experience With Several VTOL Research Aircraft.* NASA TN D-735, 1961.
2. Pegg, Robert J.: *Summary of Flight-Test Results of the VZ-2 Tilt-Wing Aircraft.* NASA TN D-989, 1962.
3. Holzhauser, Curt A.; Morello, Samuel A.; Innis, Robert C.; and Patton, James M.: *A Flight Evaluation of a VTOL Jet Transport Under Visual and Simulated Instrument Conditions.* NASA TM X-62,083, 1971.
4. Kelley, Henry L.; and Champine, Robert A.: *Flight Operating Problems and Aerodynamic and Performance Characteristics of a Fixed-Wing, Tilt-Duct, VTOL Research Aircraft.* NASA TN D-1802, 1963.
5. Koenig, David G.; Greif, Richard K.; and Kelly, Mark W.: *Full-Scale Wind-Tunnel Investigation of the Longitudinal Characteristics of a Tilting-Rotor Convertiplane.* NASA TN D-35, 1959.
6. Gibson, E. B.: The Hummingbird Program. *Proceedings of the Nineteenth Annual National Forum,* American Helicopter Soc. Inc., 1963, pp. 111–118.
7. Felker, Fort F.: An Experimental Investigation of Hub Drag on the XH-59A. AIAA-85-4065, Oct. 1985.
8. Stroub, Robert H.; Young, Larry A.; Graham, David R.; and Louie, Alexander W.: *Investigation of Generic Hub Fairing and Pylon Shapes To Reduce Hub Drag.* NASA TM-100008, 1987.
9. Bingham, Gene J.; and Noonan, Kevin W.: *Two-Dimensional Aerodynamic Characteristics of Three Rotorcraft Airfoils at Mach Numbers From 0.35 to 0.90.* NASA TP-2000, AVRADCOM TR-82-B-2, 1982.
10. Winston, Matthew M.; and Huston, Robert J.: *Wind-Tunnel Investigation of Steady-State Aerodynamics of a Composite-Lift VTOL Aircraft Model.* NASA TN D-5232, 1969.

Table I. Correlation of Run Numbers With Run Configurations

Run number	Blade chord	Blade sweep	Shaft fairing
402	Narrow	30	*
403	Narrow	0	*
406	Narrow	45	S300
407†	Narrow	30	S300
409	Narrow	30	S300
410	Narrow	0	S300
411	Wide	45	S300
412	Wide	30	S300
413	Wide	0	S300
414	Wide	0	*
415	Wide	45	*
416	Wide	30	*
417	Wide	30	S40
420	‡	‡	S40
421	‡	‡	S300
422	‡	‡	*
423	Wide	45	S40
424	Wide	0	S40

*No shaft fairing.
†Port-blade leading edge points downstream.
‡No blades.

Table II. Documented Accuracy of 842A Balance Converted to Engineering Units

Beam	Accuracy
Normal	±8.000 lb
Axial	±0.375 lb
Pitch	±15.000 in-lb
Roll	±7.500 in-lb
Yaw	±7.500 in-lb
Side	±2.500 lb

Table III. Model Geometric References To Use For Reduction of Data to Standard Coefficient Form

Configuration	S, ft^2	b, ft	$\bar{c}$, ft
No blades	5.940	2.750	2.160
Wide chord 0° sweep	7.157	5.208	1.374
Wide chord 30° sweep	7.157	4.879	1.467
Wide chord 45° sweep	7.157	4.488	1.594
Narrow chord 0° sweep	6.788	5.208	1.303
Narrow chord 30° sweep	6.788	4.879	1.391
Narrow chord 45° sweep	6.788	4.488	1.512

Table IV. Tabulated L/q and M/q Versus Angle-of-Attack Curve Slopes and Maximum Lift-to-Drag Ratios

Run number	Blade chord	Blade sweep	Shaft fairing	$(L/q)_\alpha$	$(M/q)_\alpha$	$L/D_{\max}$
402	Narrow	30	*	0.224	0.150	6.3
403	Narrow	0	*	0.252	0.216	7.3
406	Narrow	45	S300	0.208	0.157	5.6
407†	Narrow	30	S300	0.237	0.161	6.4
409	Narrow	30	S300	0.234	0.159	6.8
410	Narrow	0	S300	0.262	0.220	7.9
411	Wide	45	S300	0.217	0.150	5.7
412	Wide	30	S300	0.263	0.144	6.8
413	Wide	0	S300	0.320	0.227	8.4
414	Wide	0	*	0.302	0.220	7.9
415	Wide	45	*	0.203	0.151	5.6
416	Wide	30	*	0.235	0.139	6.6
417	Wide	30	S40	0.262	0.142	6.5
420	‡	‡	S40	0.157	0.202	4.6
421	‡	‡	S300	0.162	0.206	4.9
422	‡	‡	*	0.149	0.198	4.7
423	Wide	45	S40	0.217	0.149	5.3
424	Wide	0	S40	0.316	0.231	8.0

*No shaft fairing.
†Port-blade leading edge points downstream.
‡No blades.

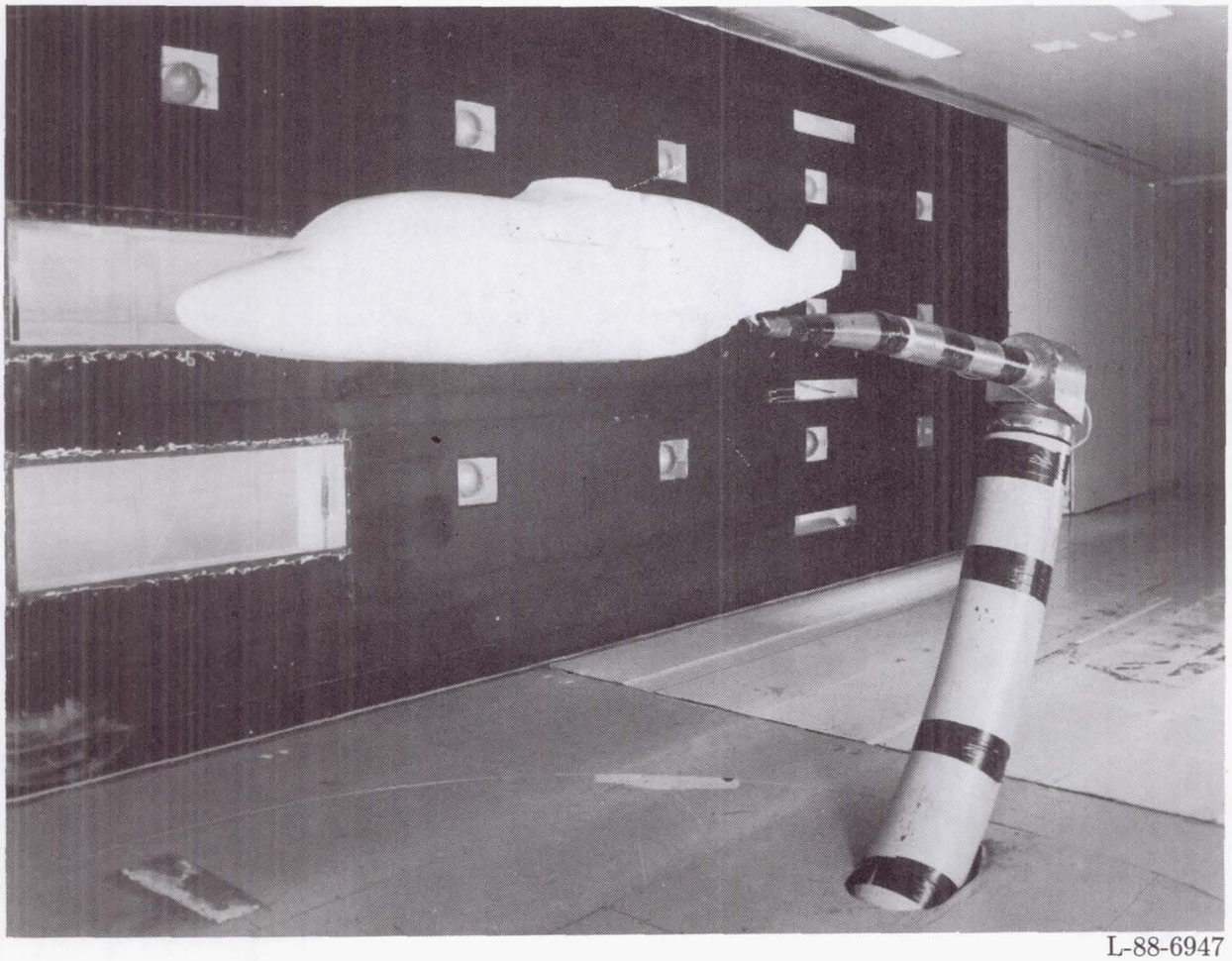

L-88-6947

Figure 1. One-fifth scale XH-59A advancing blade concept fuselage model sting-mounted in the Langley 14- by 22-Foot Subsonic Tunnel.

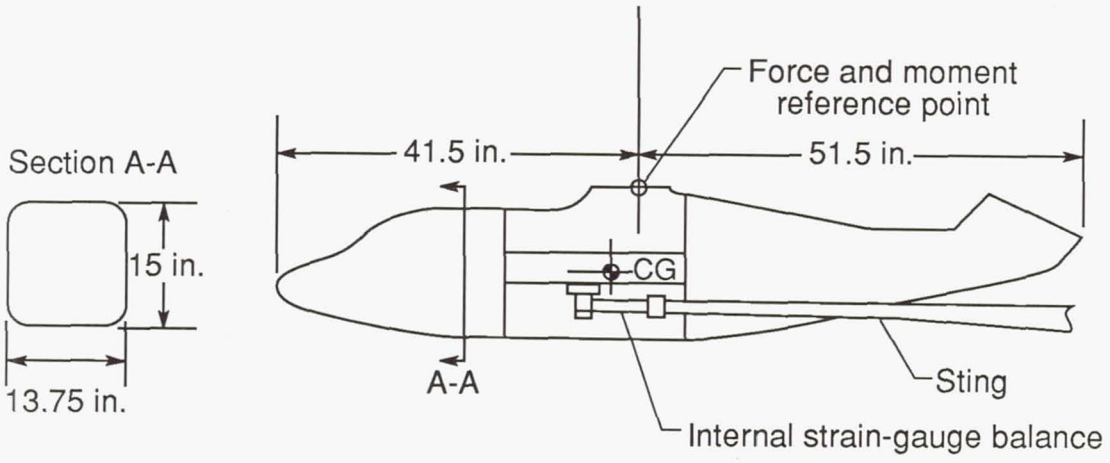

Figure 2. Model dimensions and mounting scheme.

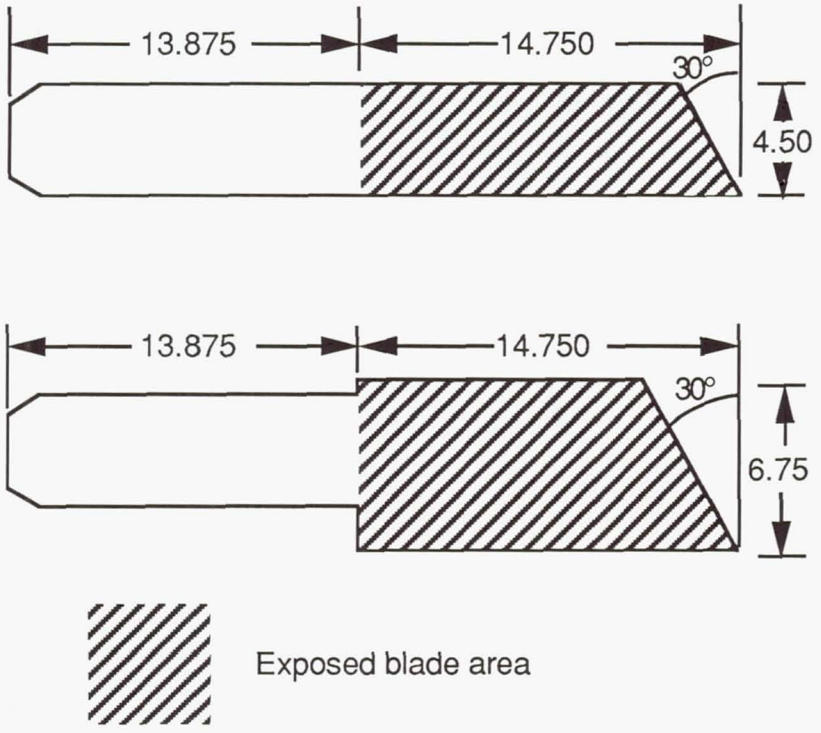

Figure 3. Sketch of blade set planforms. (Linear dimensions in inches.)

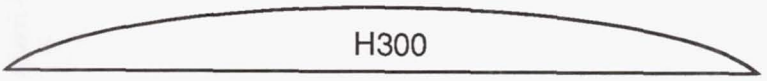

Diameter, in.	33.00
Thickness ratio	0.11
Camber	0.05

Figure 4. Side view cross section and geometric properties of H300 hub fairing.

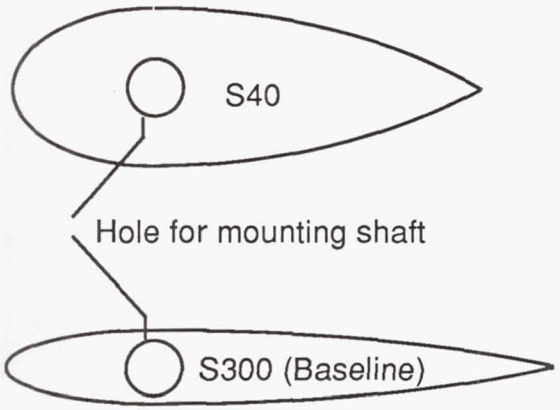

	S40	S300
Chord length, in.	19.00	20.00
Thickness ratio	0.34	0.15
Location of maximum thickness	0.30	0.30
Trailing-edge slope	-1.17	-0.18
Height, in.	2.00	2.00

Figure 5. Top view cross sections and geometric properties of the S40 and S300 (baseline) shaft fairings.

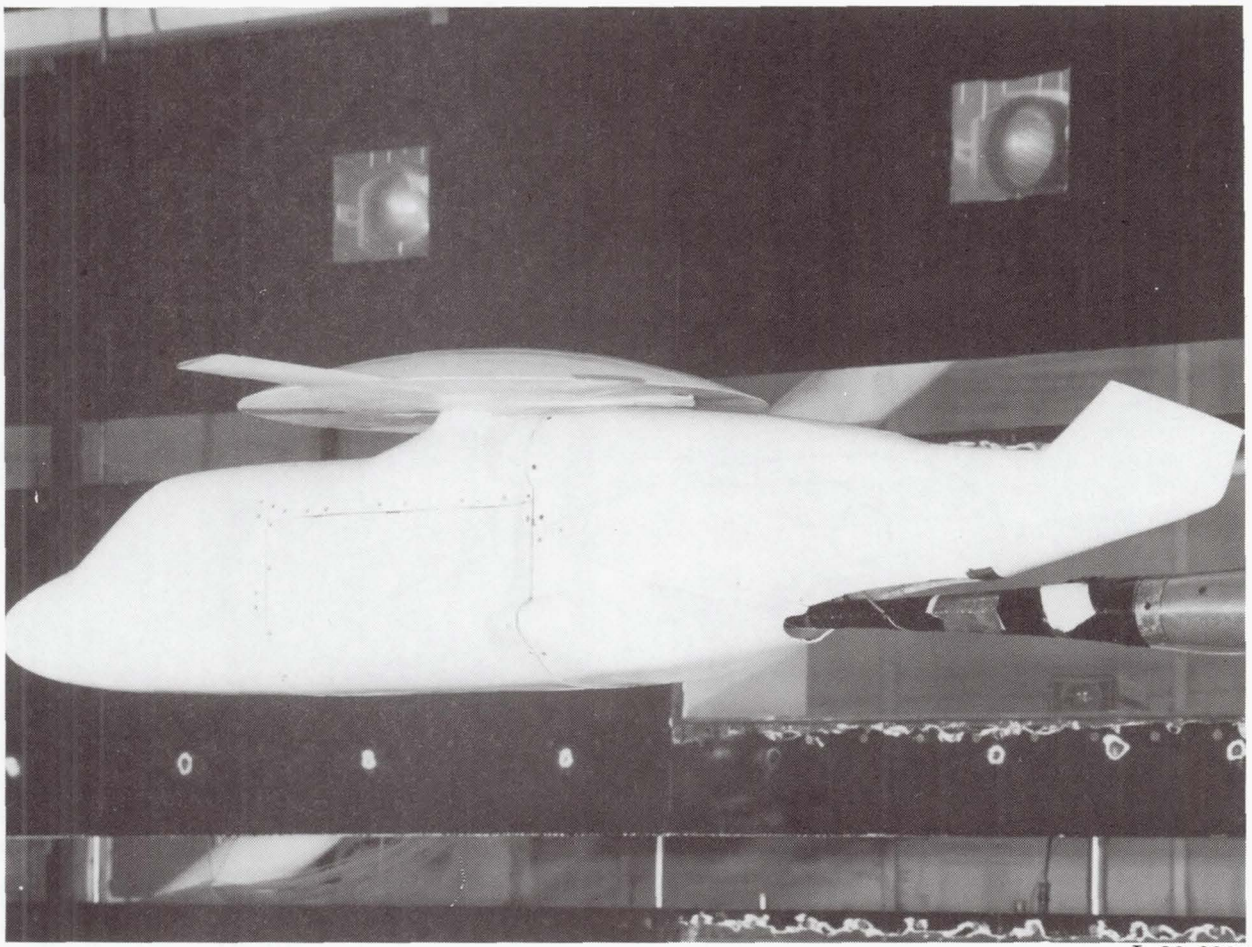

L-88-6801

Figure 6. A typical M85 run configuration. Wide-chord blades on the hub fairing mounted on the fuselage model.

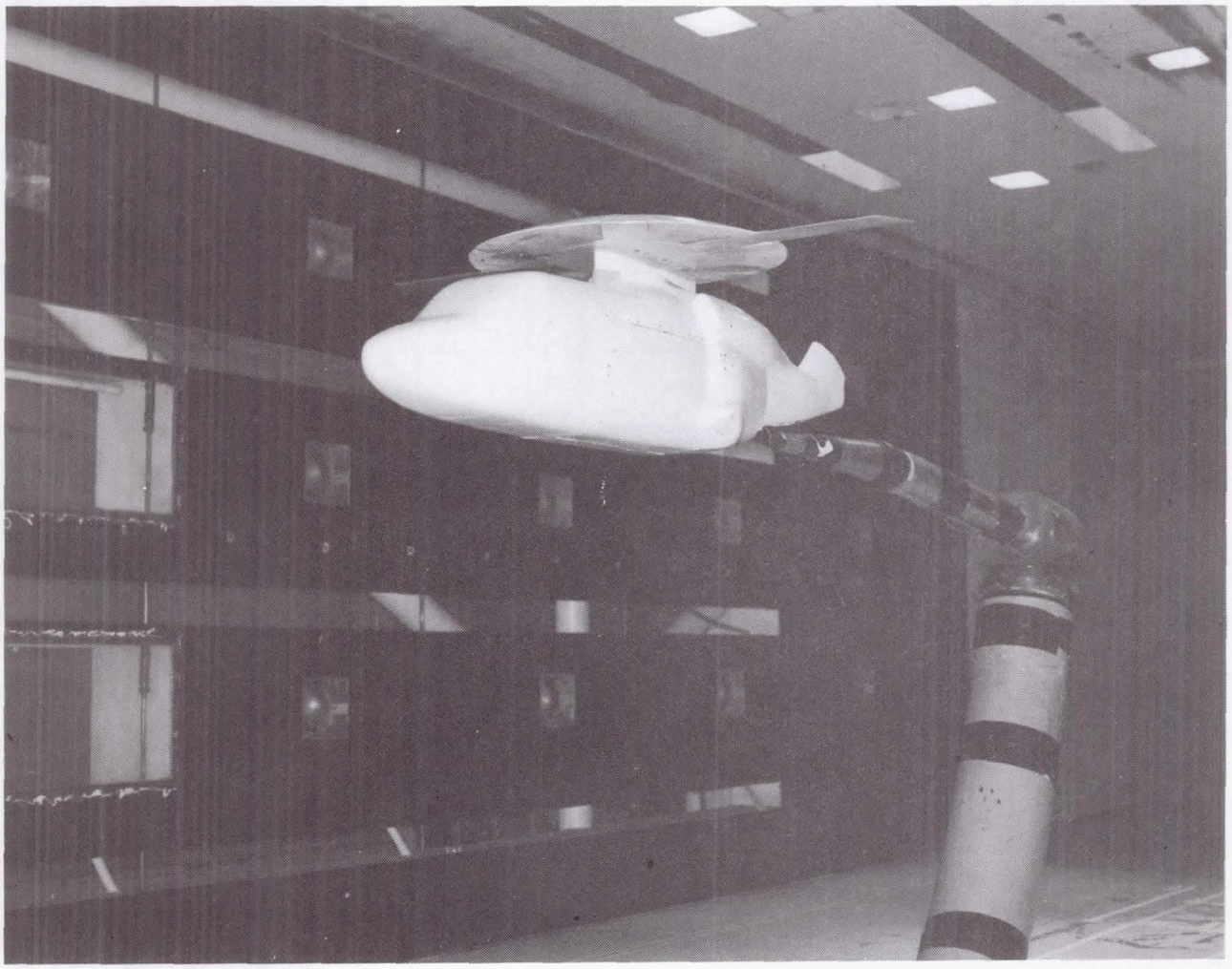

Figure 7. Baseline configuration: 1/5-scale model XH-59A fuselage with S300 shaft fairing, H300 hub fairing, and wide-chord blades at a sweep angle of 0°.

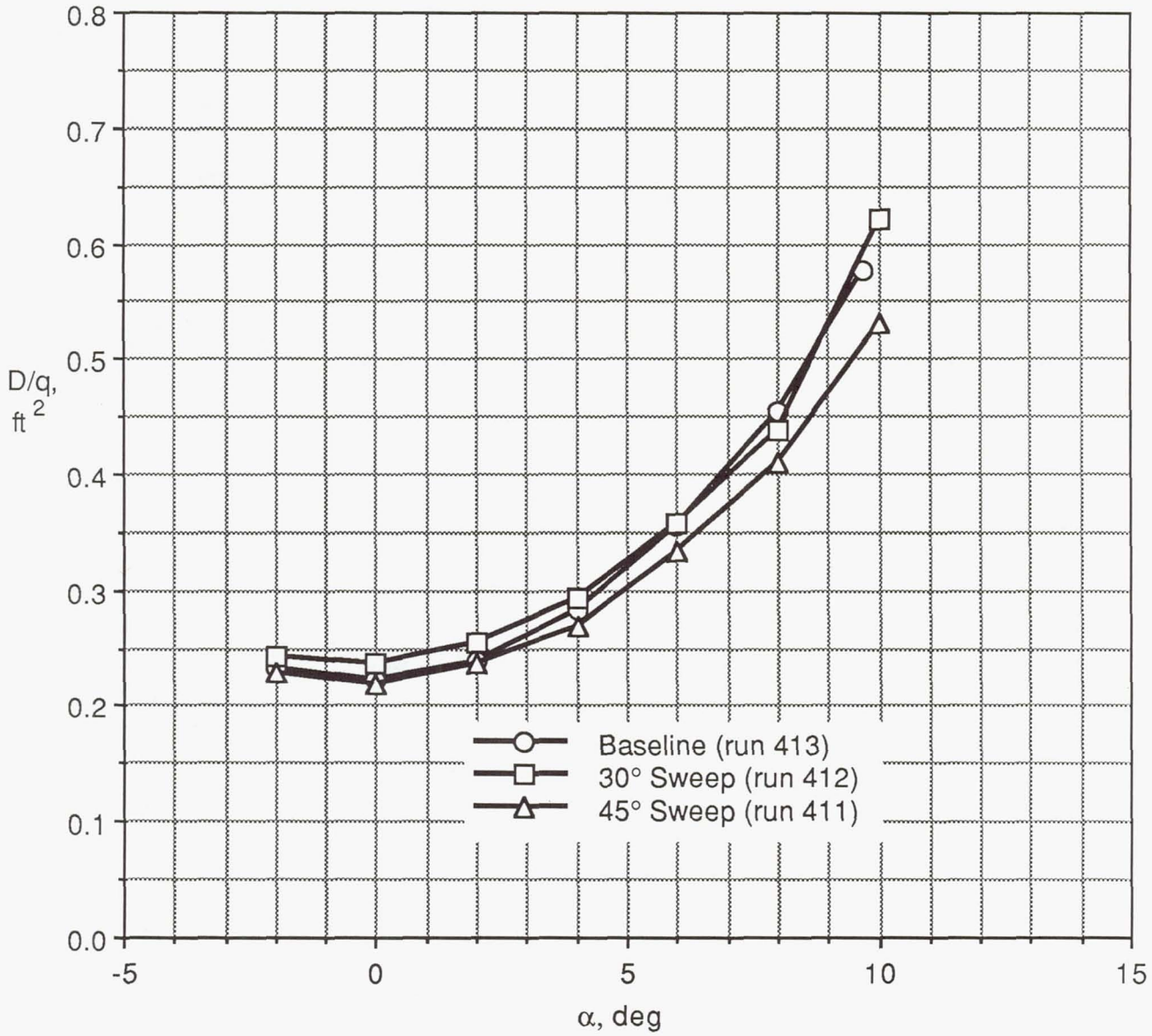

(a) Drag.

Figure 8. Effect of blade sweep on M85 aerodynamic characteristics: S300 shaft fairing, wide-chord configuration.

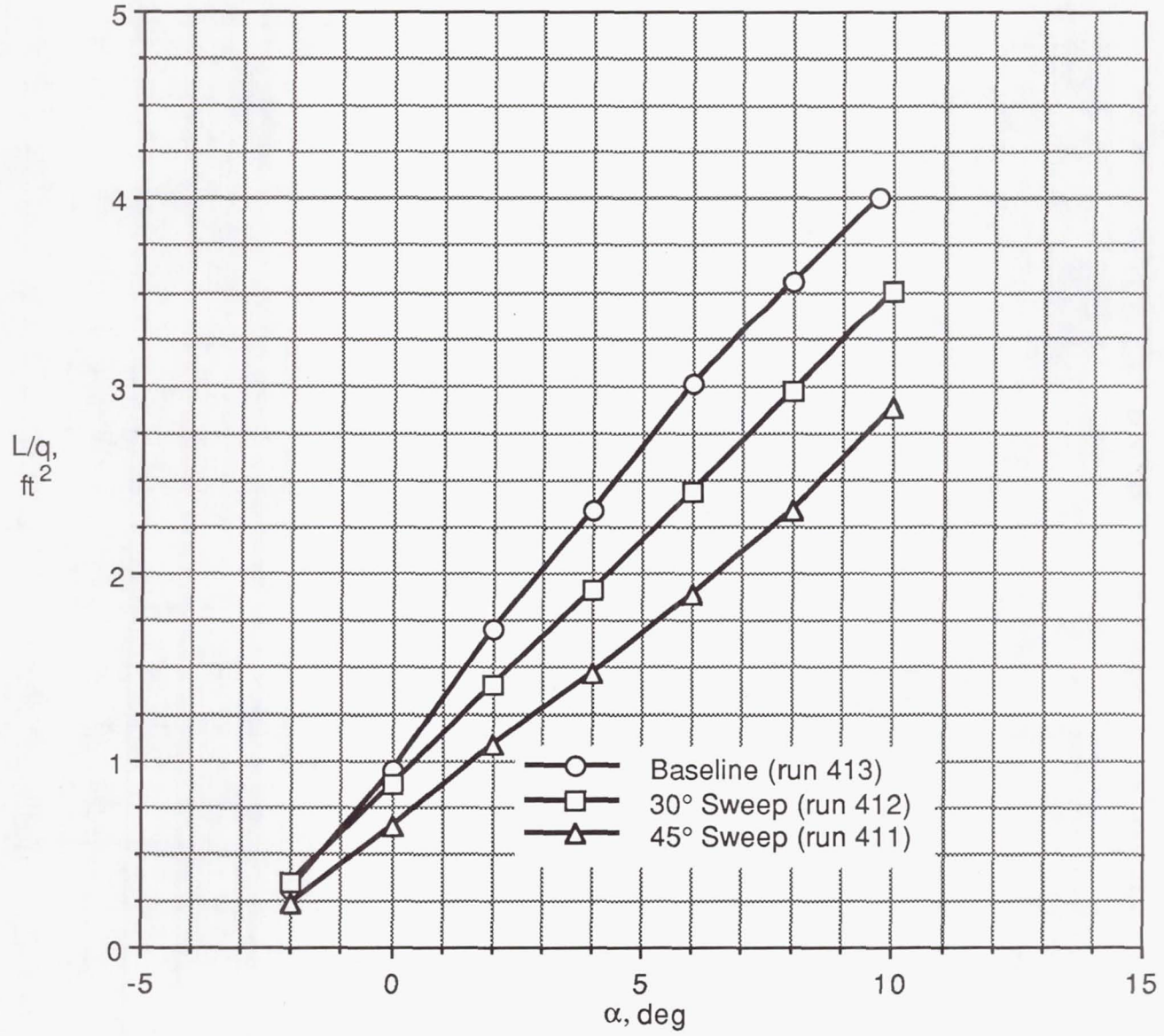

(b) Lift.

Figure 8. Continued.

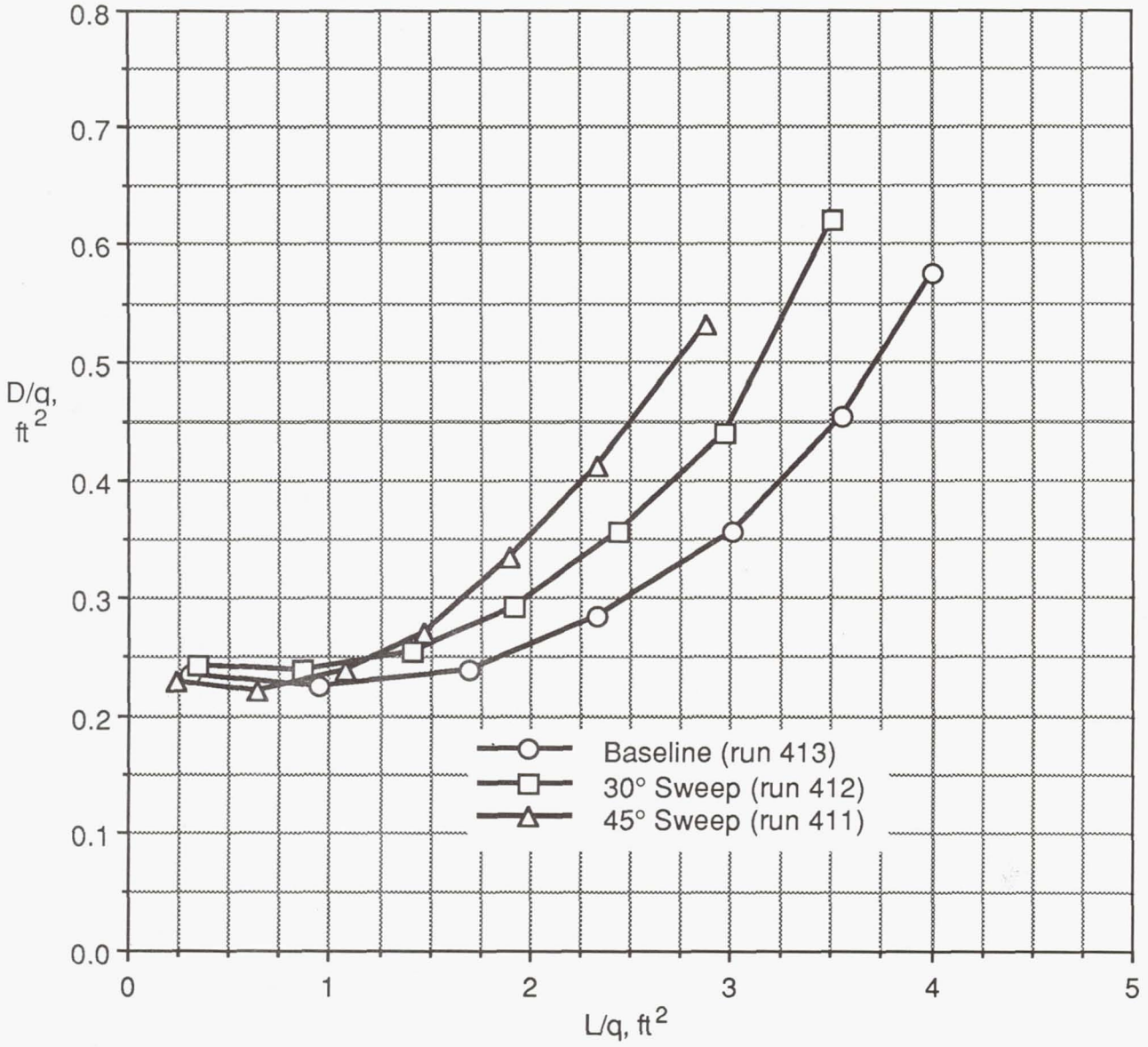

(c) Efficiency.

Figure 8. Continued.

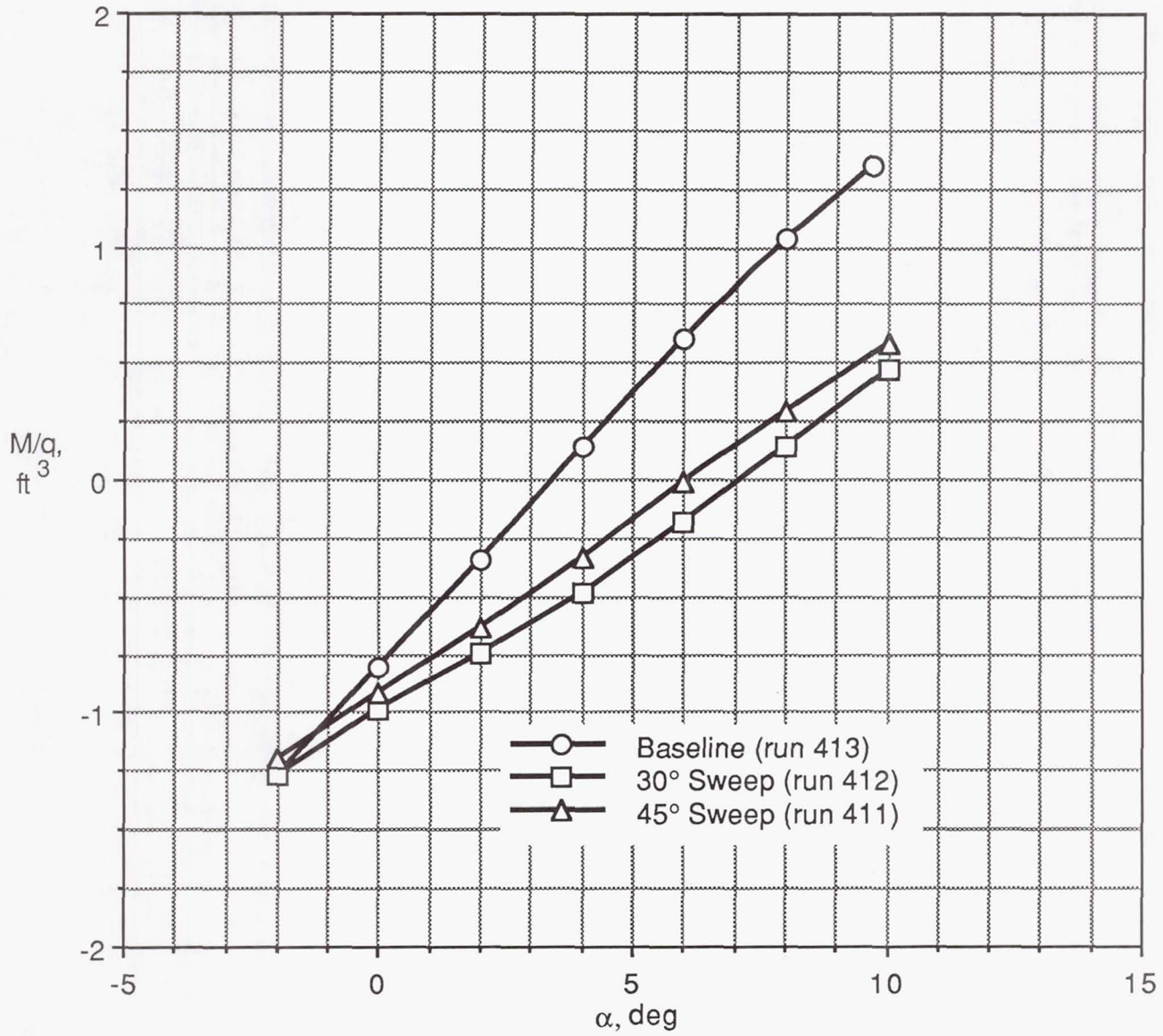

(d) Stability.

Figure 8. Concluded.

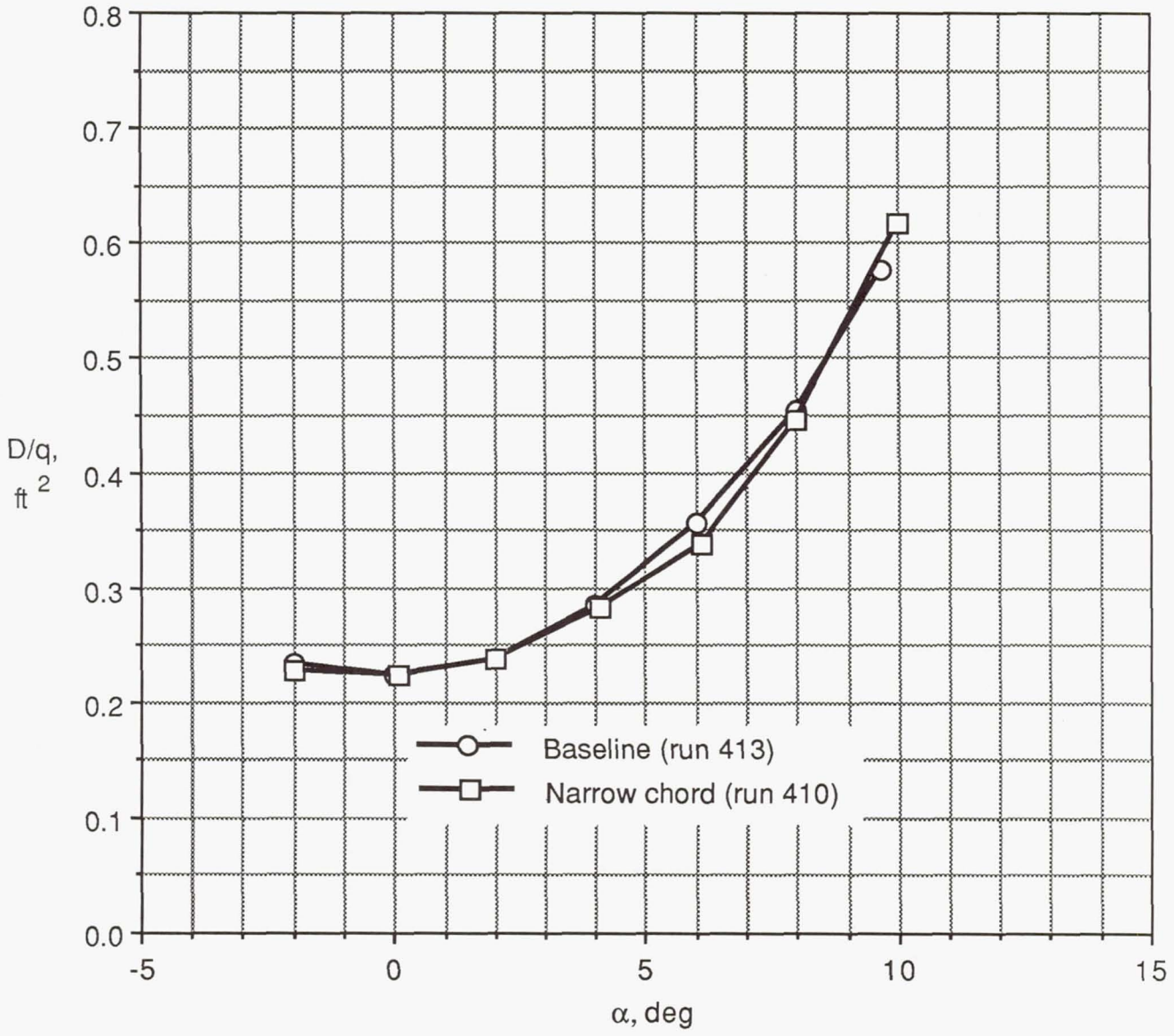

(a) Drag.

Figure 9. Effect of blade chord on M85 aerodynamic characteristics: S300 shaft fairing, sweep configuration of 0°.

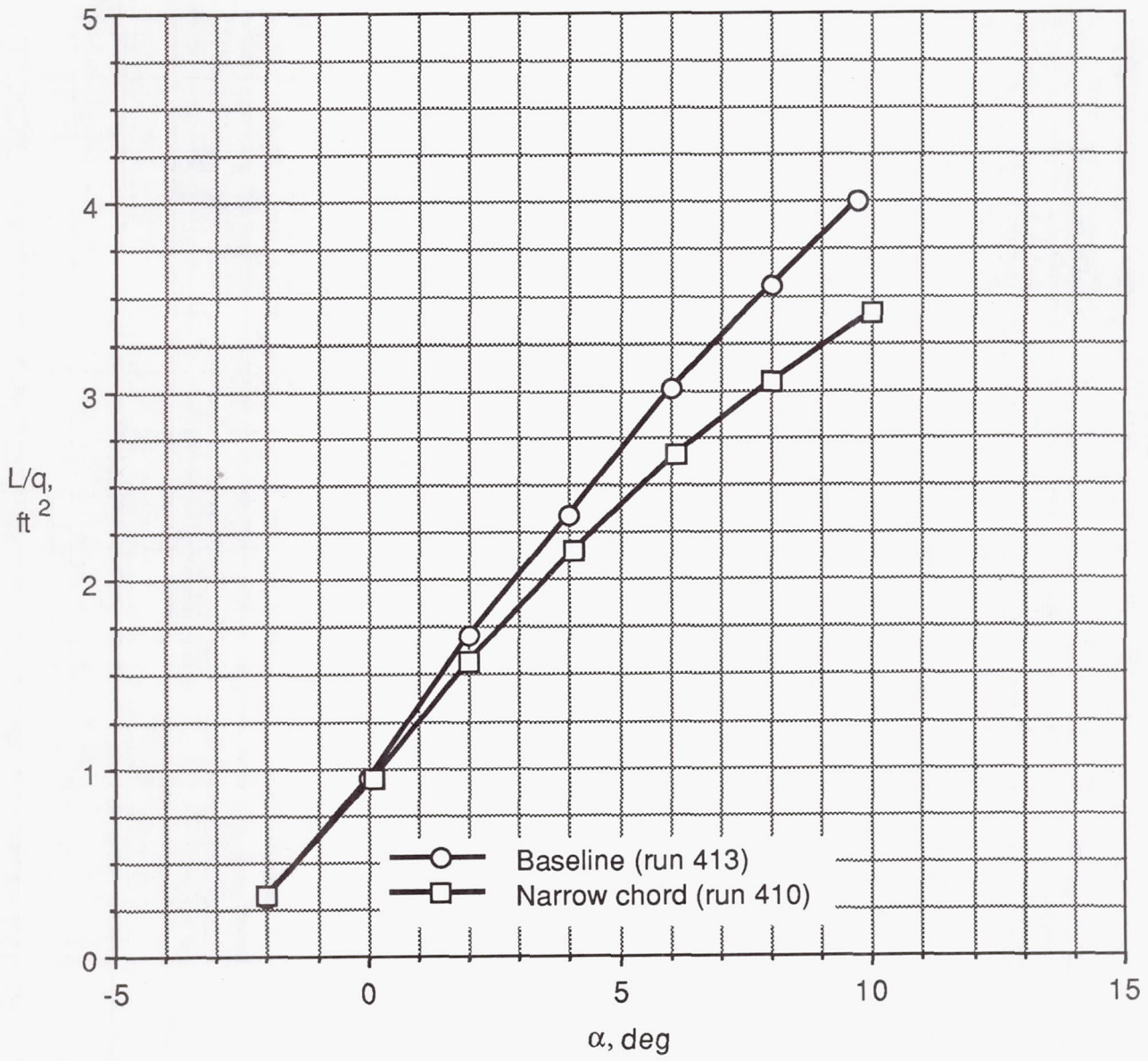

(b) Lift.

Figure 9. Continued.

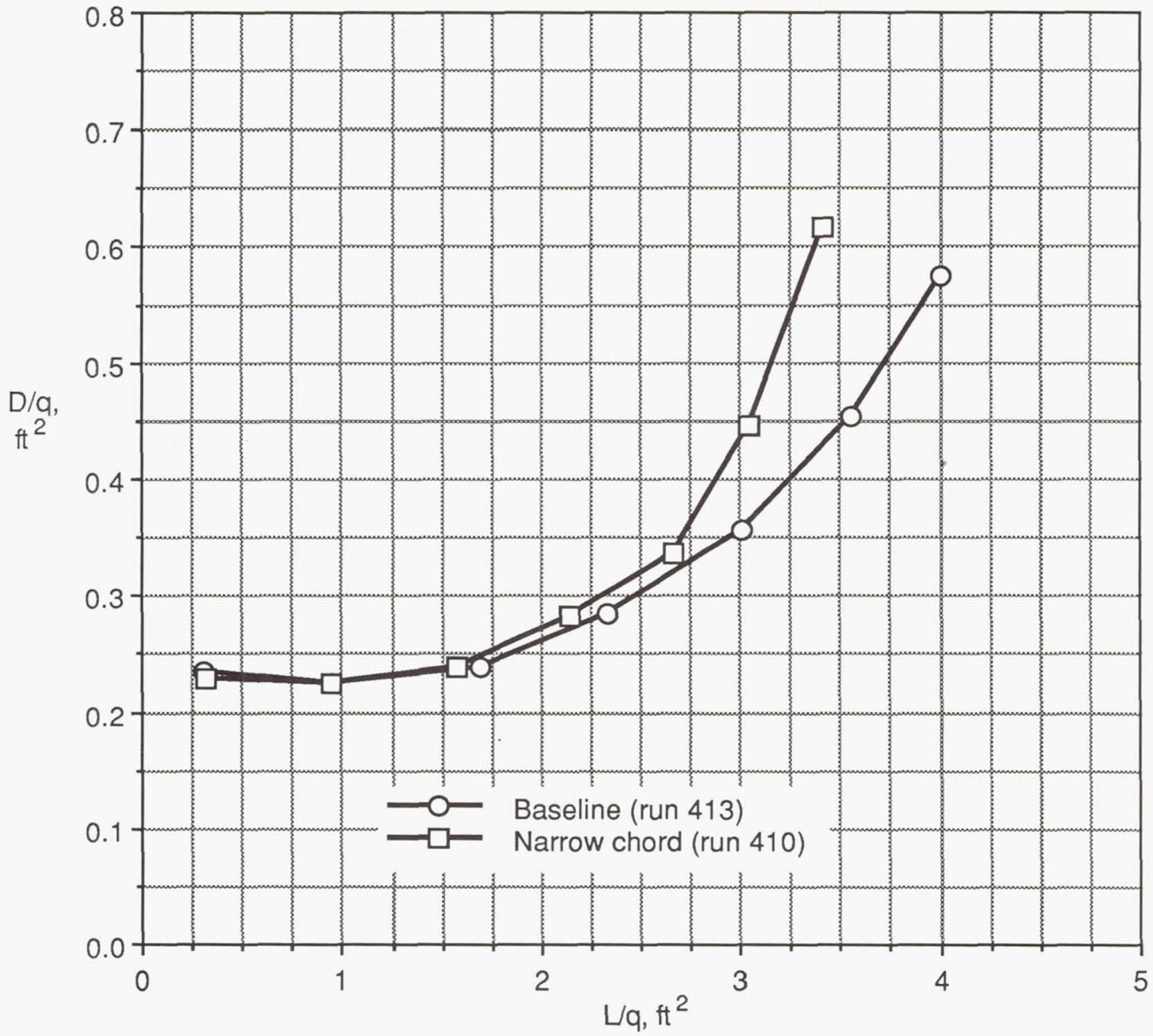

(c) Efficiency.

Figure 9. Continued.

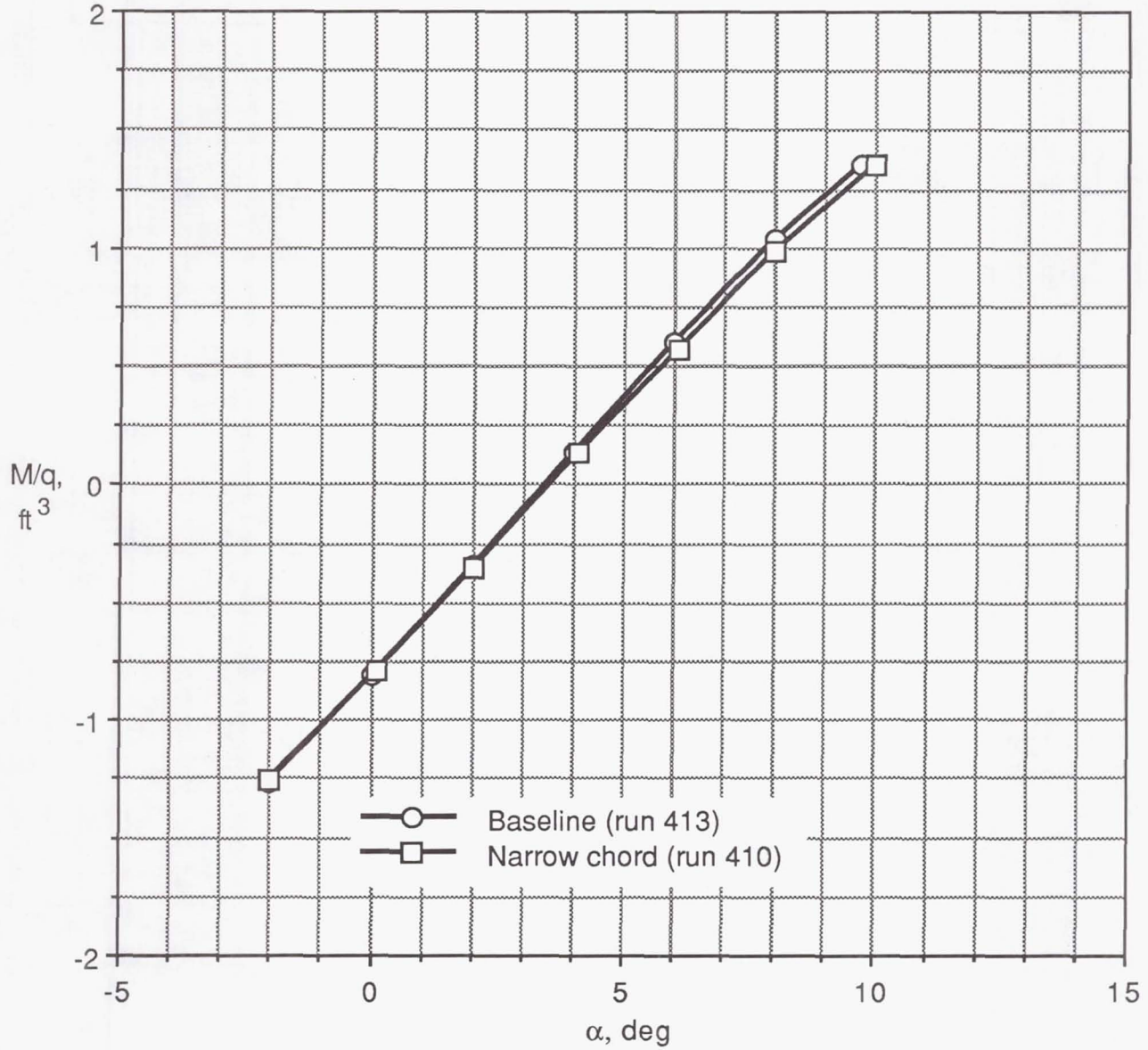

(d) Stability.

Figure 9. Concluded.

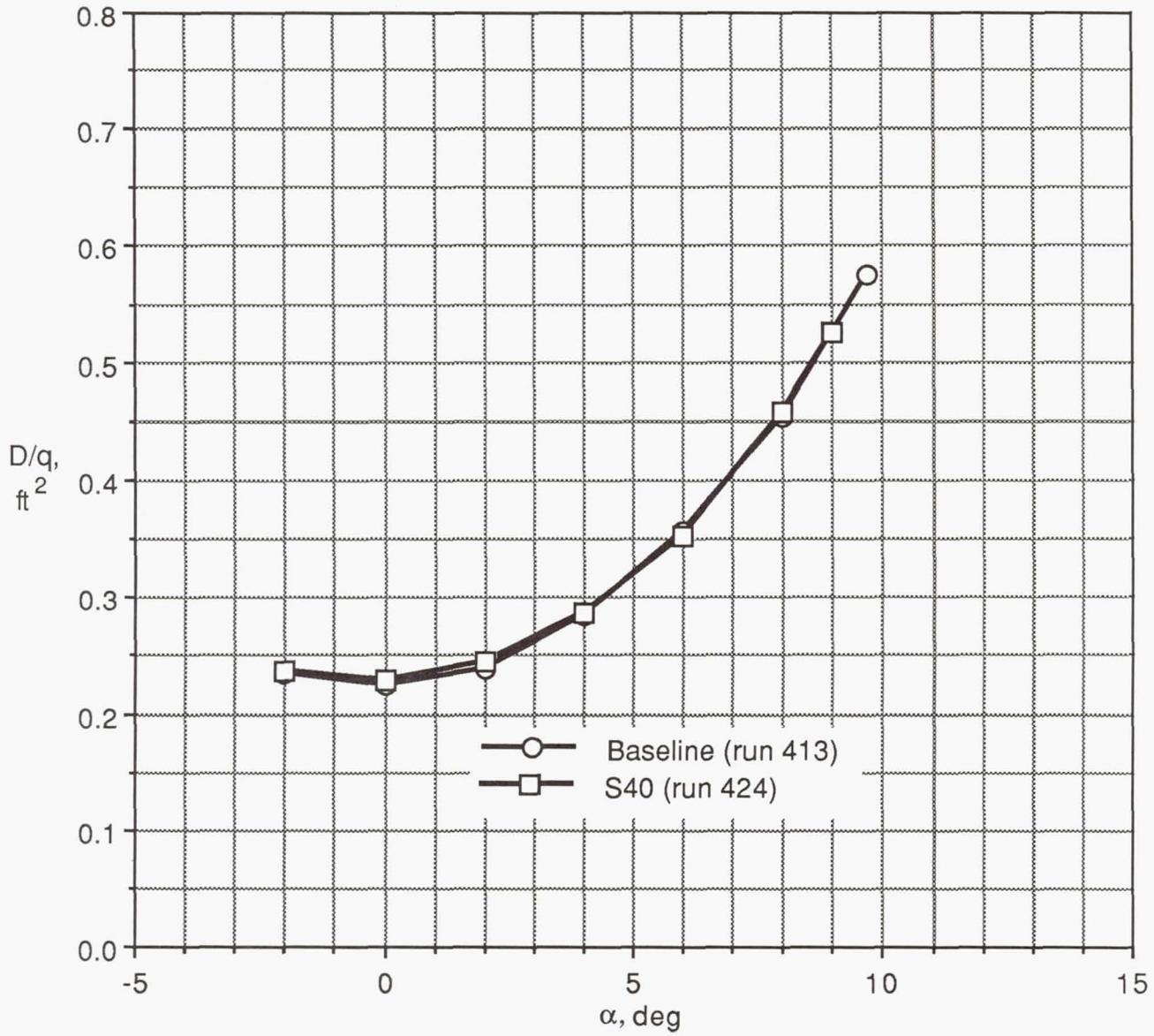

(a) Drag.

Figure 10. Effect of shaft fairing geometry on M85 aerodynamic characteristics: sweep angle of 0°, wide-chord configuration.

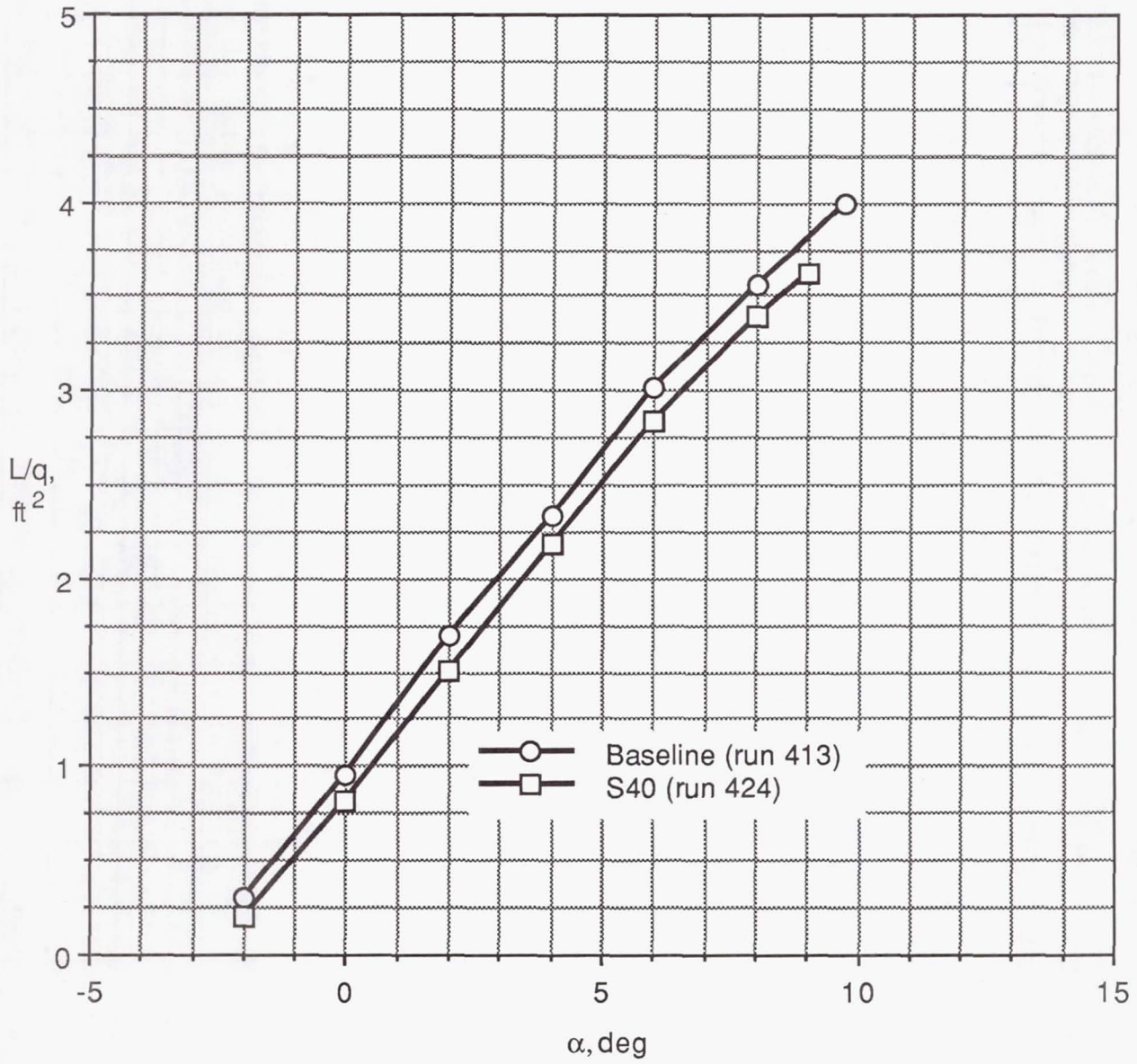

(b) Lift.

Figure 10. Continued.

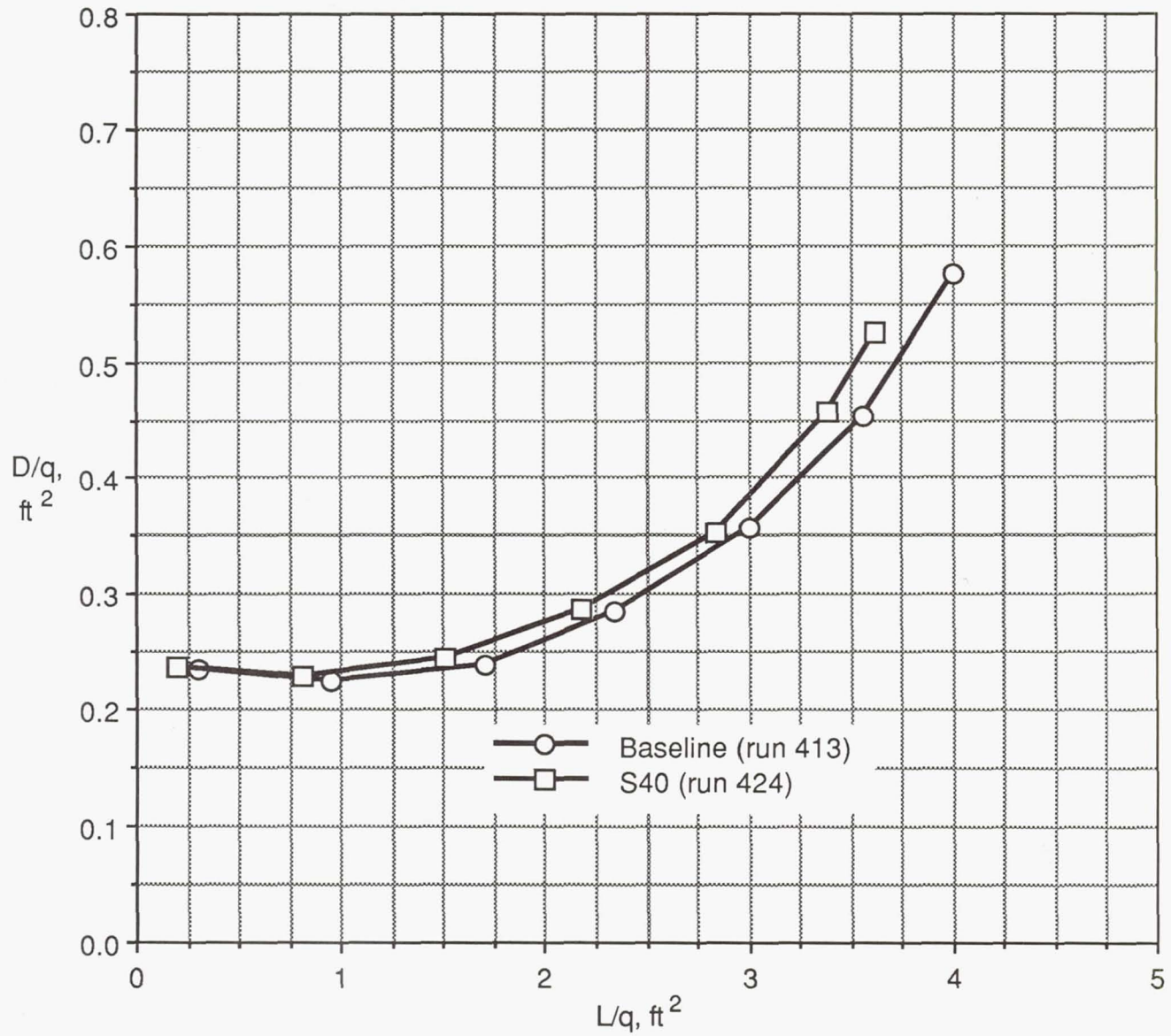

(c) Efficiency.

Figure 10. Continued.

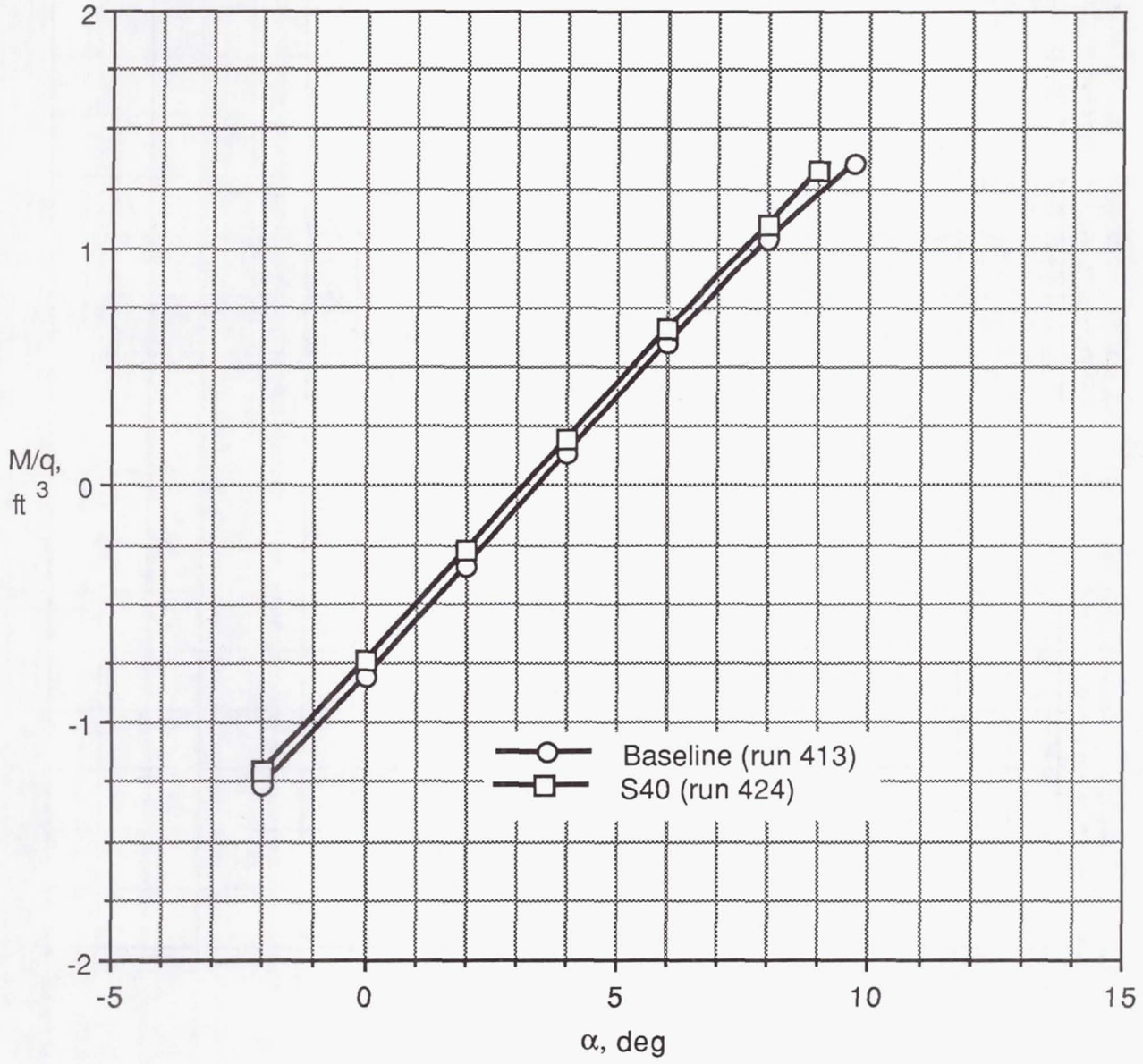

(d) Stability.

Figure 10. Concluded.

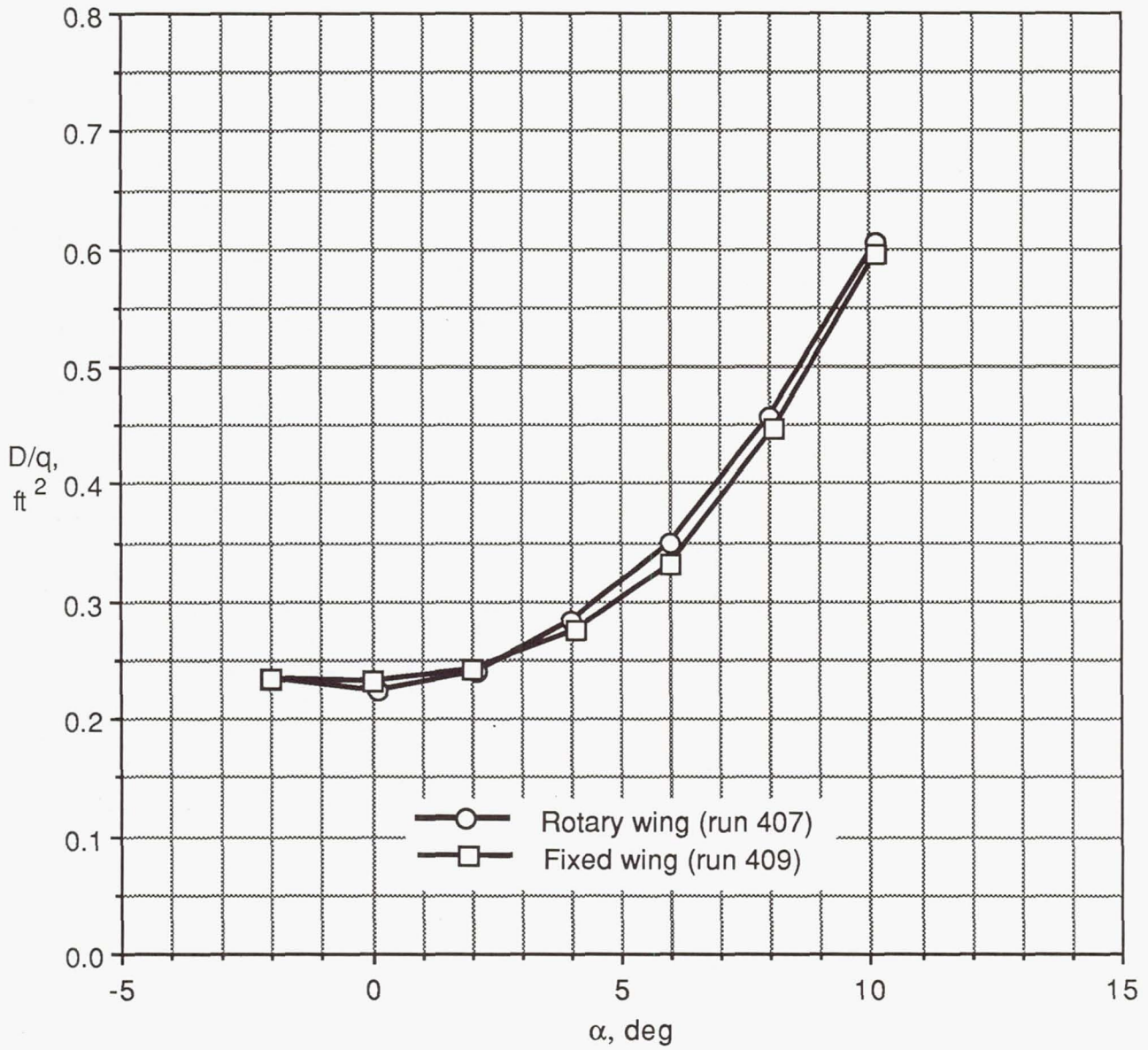

(a) Drag.

Figure 11. Effect of port-blade leading-edge orientation on M85 aerodynamic characteristics: S300 shaft fairing, sweep angle of 0°, wide-chord configuration.

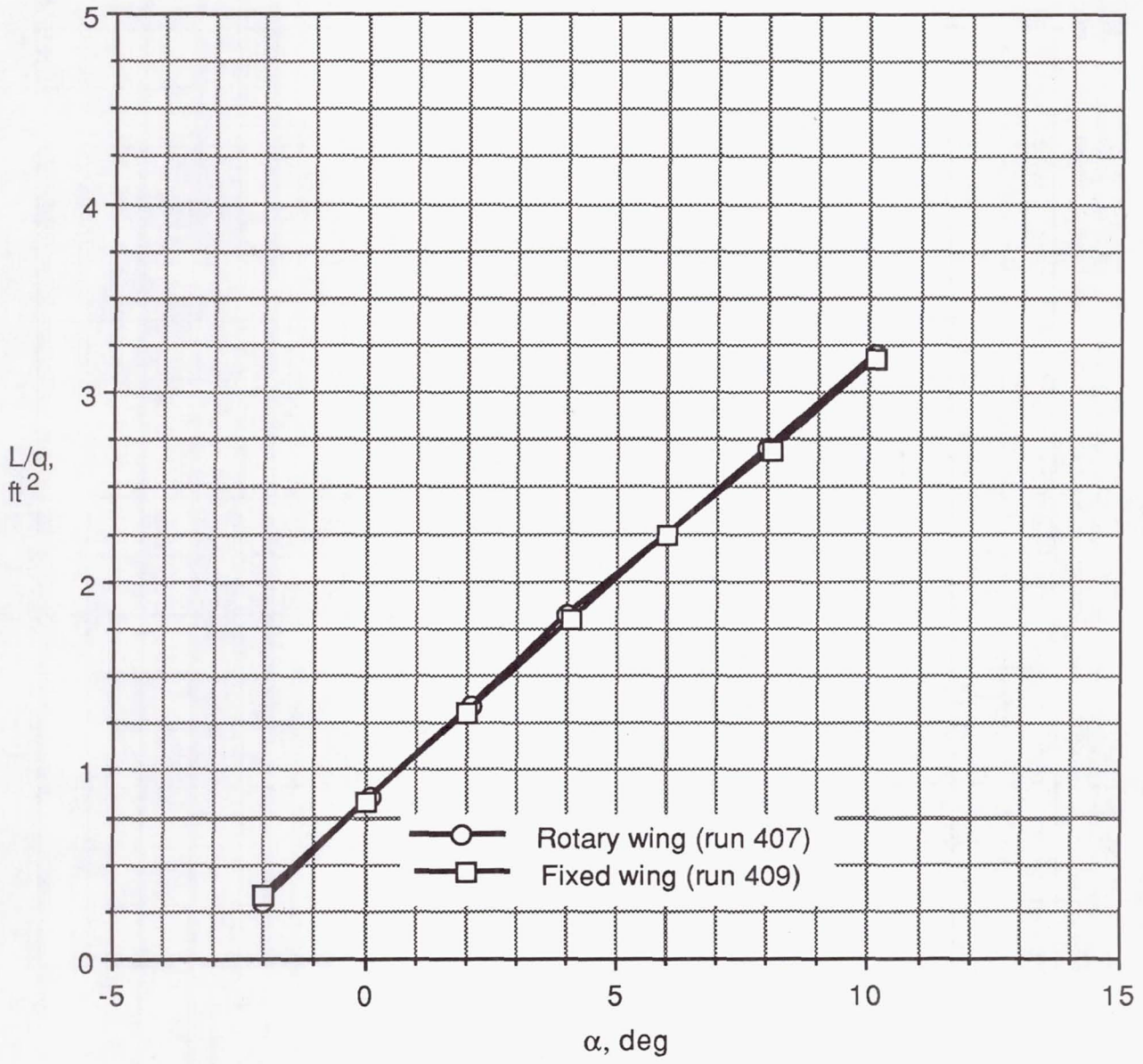

(b) Lift.

Figure 11. Continued.

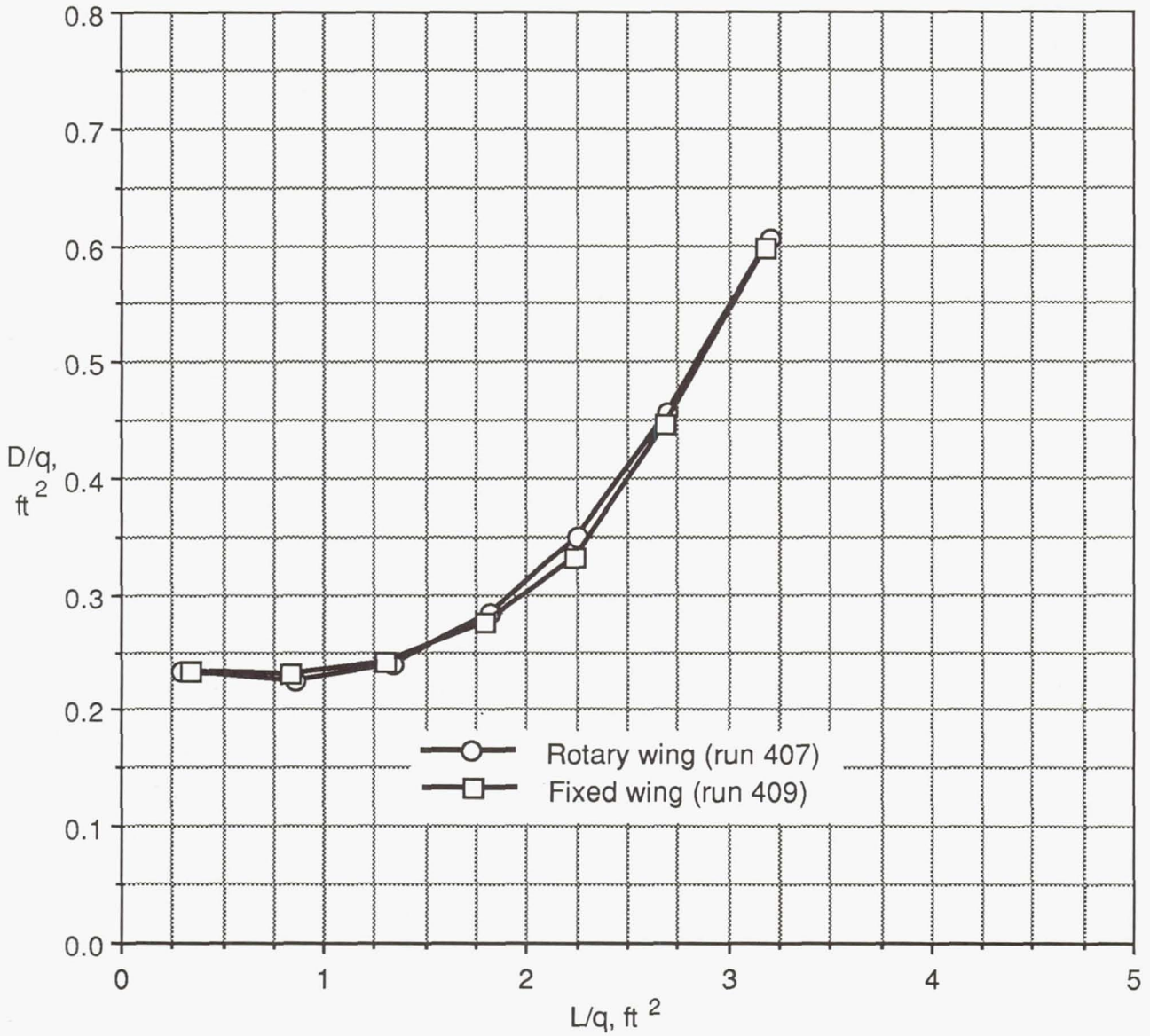

(c) Efficiency.

Figure 11. Continued.

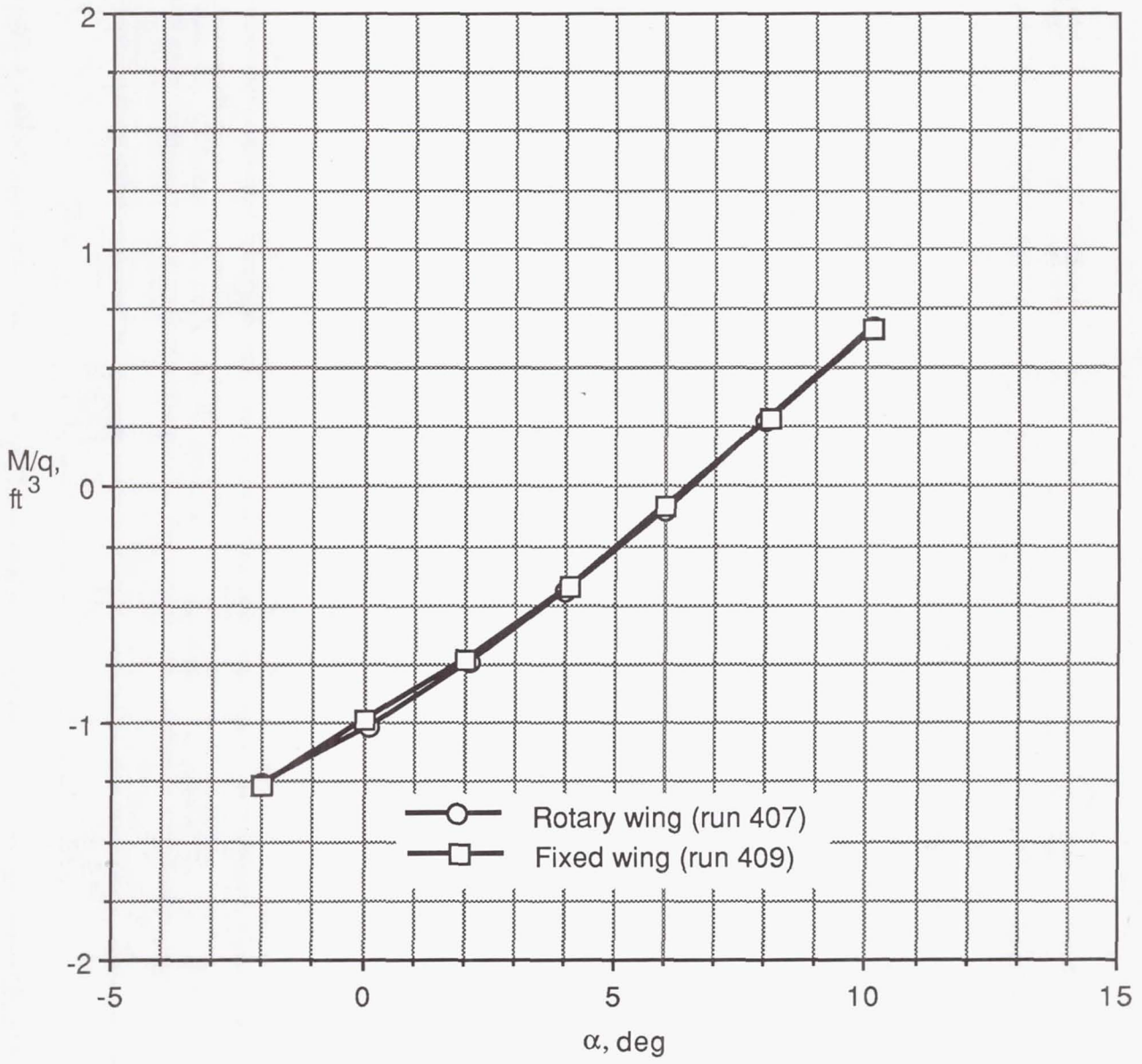

(d) Stability.

Figure 11. Concluded.

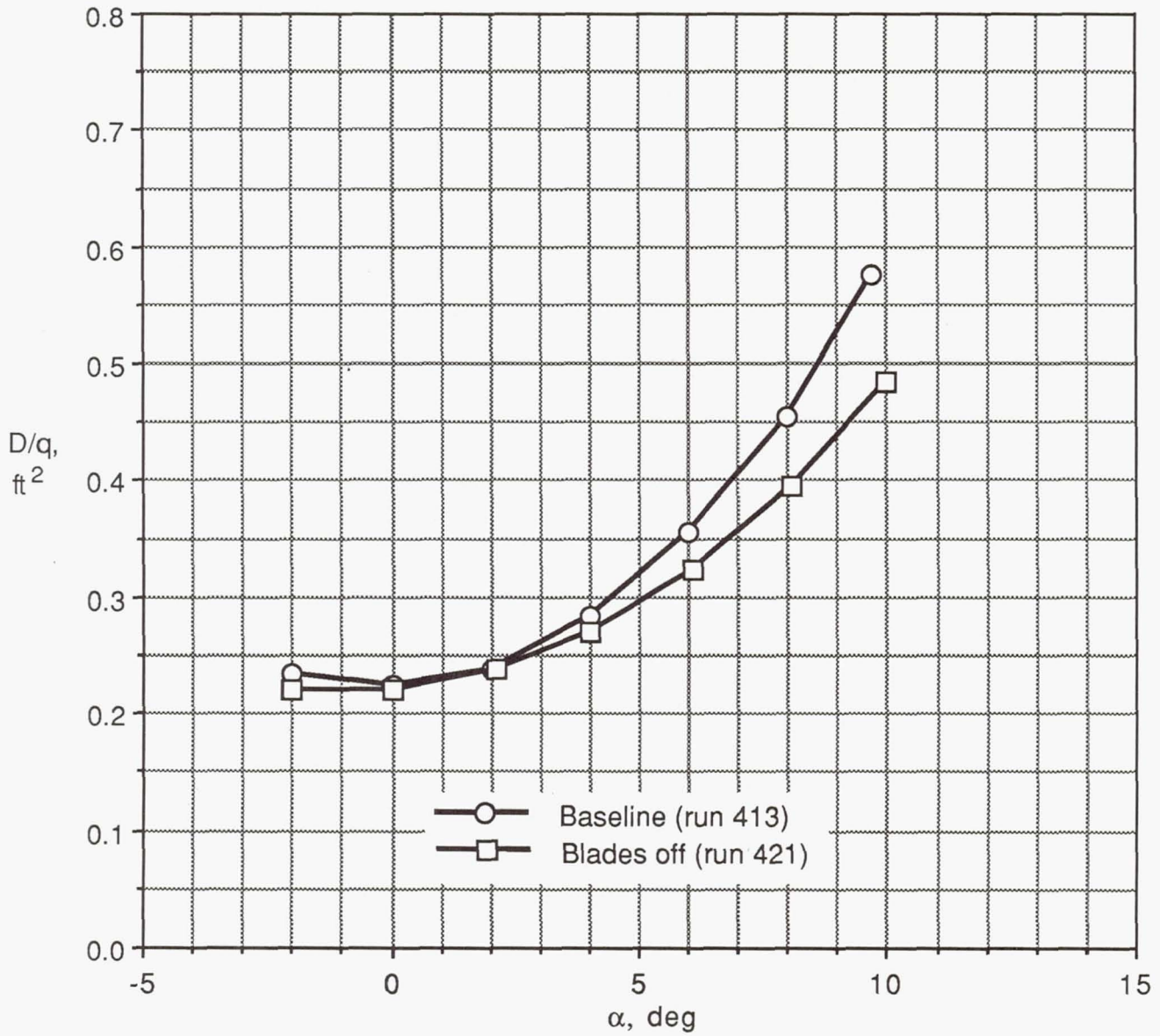

(a) Drag.

Figure 12. Aerodynamic characteristics of the M85 in a bladeless configuration.

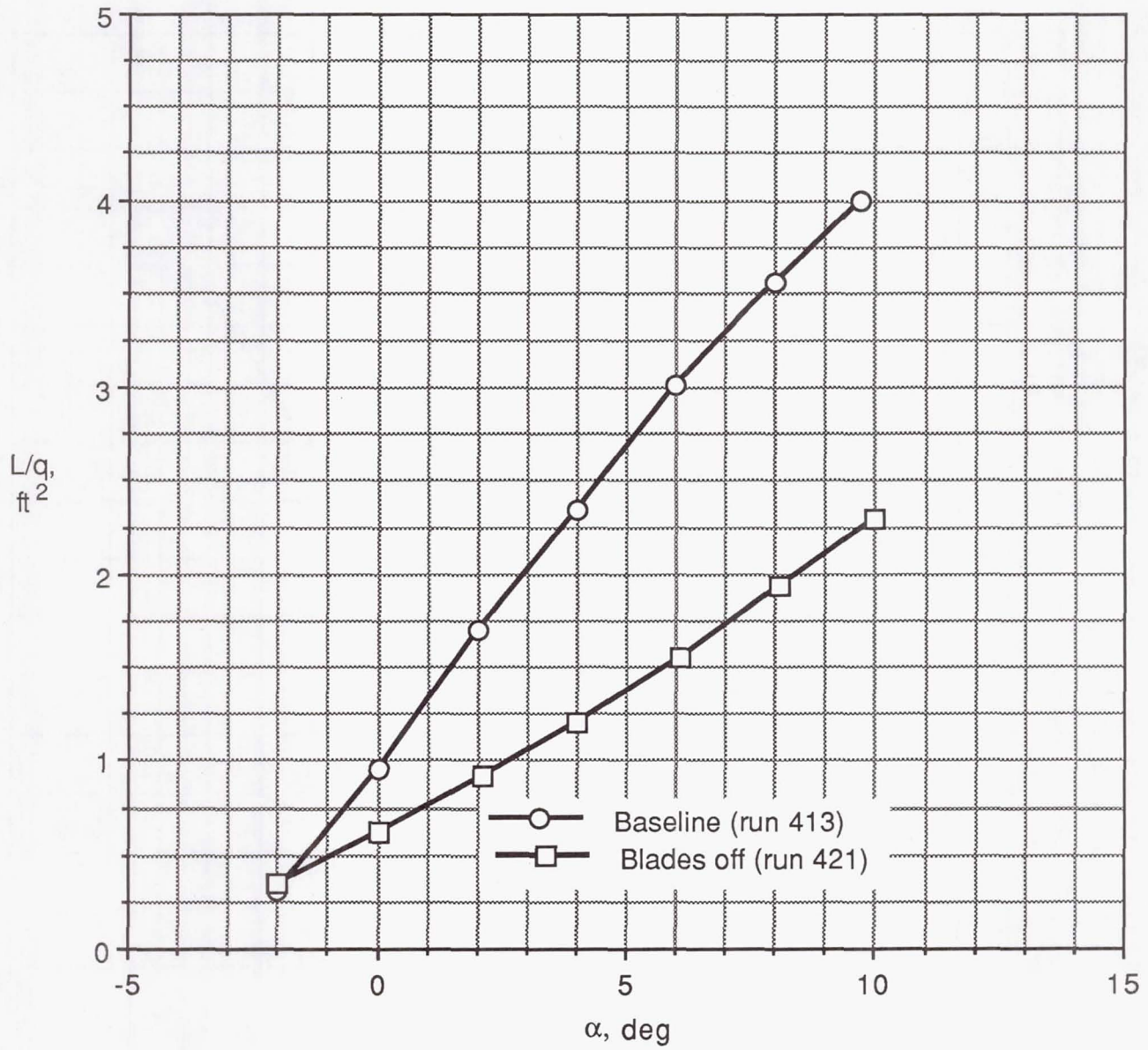

(b) Lift.

Figure 12. *Continued.*

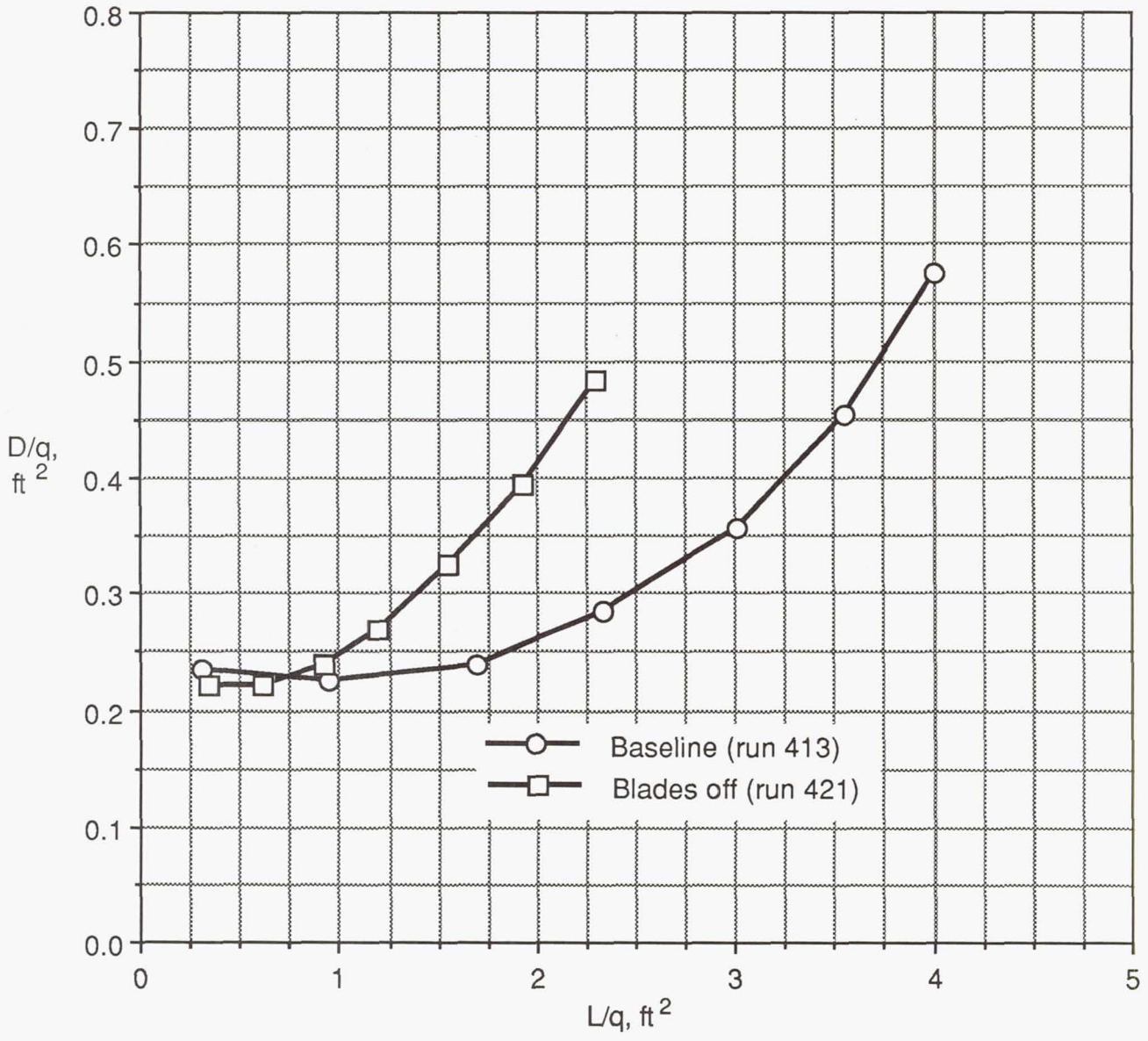

(c) Efficiency.

Figure 12. Continued.

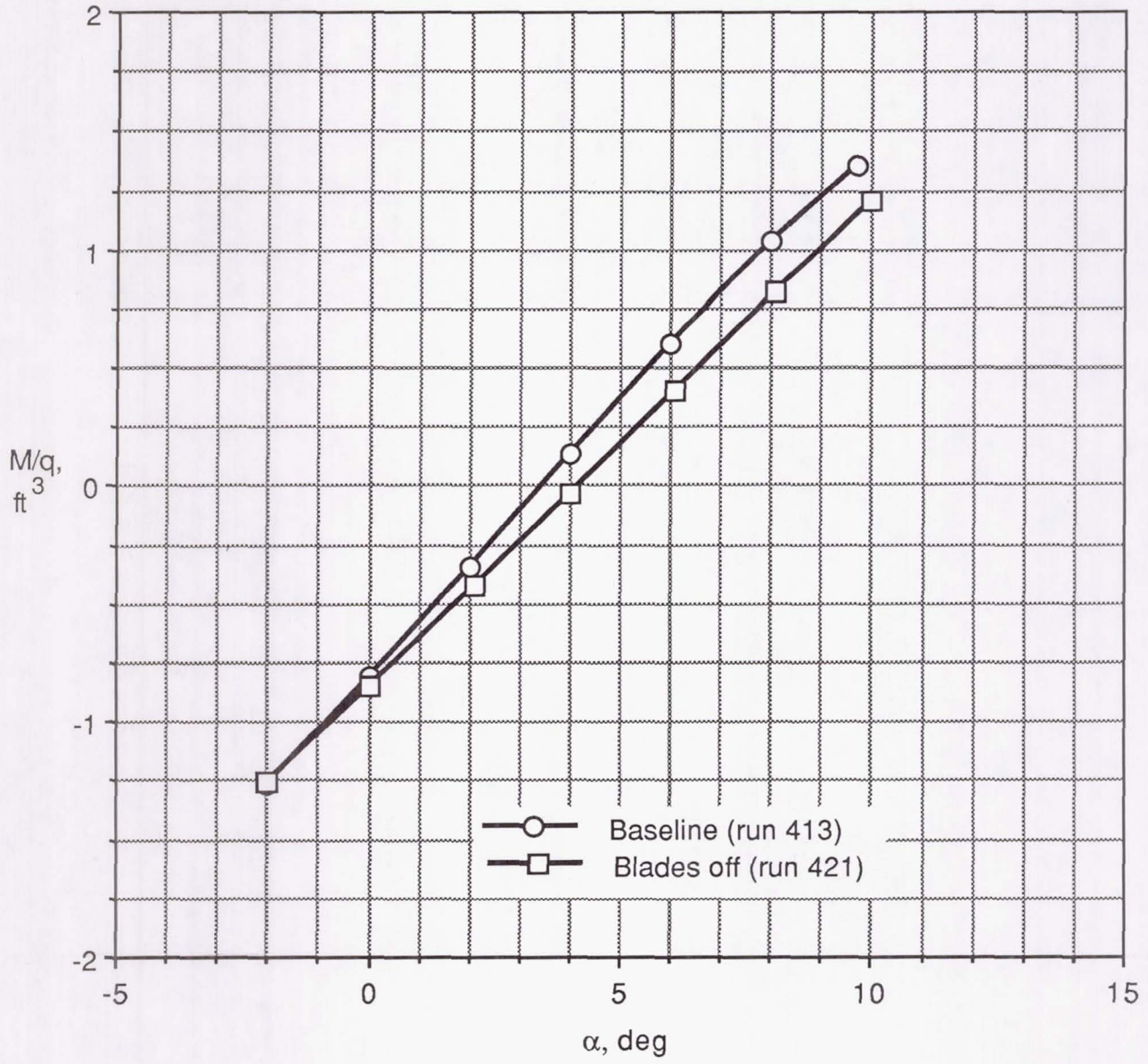

(d) Stability.

Figure 12. Concluded.

NASA
National Aeronautics and Space Administration

Report Documentation Page

1. Report No.	2. Government Accession No.	3. Recipient's Catalog No.
NASA TM-4250		

4. Title and Subtitle	5. Report Date
Low-Speed Wind-Tunnel Test of an Unpowered High-Speed Stoppable Rotor Concept in Fixed-Wing Mode	March 1991
	6. Performing Organization Code
7. Author(s)	8. Performing Organization Report No.
Michael B. Lance, Daniel Y. Sung, and Robert H. Stroub	L-16716
9. Performing Organization Name and Address	10. Work Unit No.
NASA Langley Research Center Hampton, VA 23665-5225	505-61-51-10
	11. Contract or Grant No.
12. Sponsoring Agency Name and Address	13. Type of Report and Period Covered
National Aeronautics and Space Administration Washington, DC 20546-0001	Technical Memorandum
	14. Sponsoring Agency Code

15. Supplementary Notes

Michael B. Lance: Lockheed Engineering & Sciences Company, Hampton, Virginia.
Daniel Y. Sung: Sterling Software, Palo Alto, California.
Robert H. Stroub: Ames Research Center, Moffett Field, California.

16. Abstract

An experimental investigation of the M85, a high-speed rotor concept, was conducted in the Langley 14- by 22-Foot Subsonic Tunnel in cooperation with NASA Ames Research Center. An unpowered 1/5-scale model of the XH-59A helicopter fuselage with a large circular hub fairing, two rotor blades, and a shaft fairing was used as a baseline configuration. The M85 is a rotor-wing hybrid aircraft design, and the model was tested with the rotor blades in the fixed-wing mode. Assessments of the aerodynamic characteristics of various model rotor configurations were made. Variations in configuration were produced by changing the rotor blade sweep angle and the blade chord length. The most favorable M85 configuration tested included wide-chord blades at a sweep angle of 0°; the configuration attained a system lift-to-drag ratio of 8.4.

17. Key Words (Suggested by Authors(s))	18. Distribution Statement
Helicopters High-speed rotorcraft Compound helicopters Wind-tunnel testing Circular wing	Unclassified—Unlimited Subject Category 02

19. Security Classif. (of this report)	20. Security Classif. (of this page)	21. No. of Pages	22. Price
Unclassified	Unclassified	52	A04

NASA FORM 1626 OCT 86

NASA-Langley, 1991

For sale by the National Technical Information Service, Springfield, Virginia 22161-2171